Quaternary Science Reviews 309 (2023) 108033

Contents lists available at ScienceDirect

Quaternary Science Reviews

journal homepage: www.elsevier.com/locate/quascirev

An archaeostratigraphic consideration of the Gran Dolina TD10.2 cultural sequence from a quantitative approach

Andion Arteaga-Brieba [a, b, *], Lloyd A. Courtenay [c, d], Lucía Cobo-Sánchez [e], Antonio Rodríguez-Hidalgo [a, b], Palmira Saladié [a, b, f], Andreu Ollé [a, b], Marina Mosquera [a, b]

[a] Universitat Rovira i Virgili (URV), Departament d'Història i Història de l'Art, Avinguda de Catalunya 35, 43002, Tarragona, Spain
[b] Institut Català de Paleoecologia Humana i Evolució Social (IPHES-CERCA), Zona Educacional 4, Campus Sescelades URV (Edifici W3), 43007, Tarragona, Spain
[c] Department of Cartographic and Land Engineering, Higher Polytechnic School of Ávila, University of Salamanca, Hornos Caleros 50, 05003, Ávila, Spain
[d] Department of Prehistory, Ancient History and Archaeology, Complutense University of Madrid, Prof. Aranguren s/n, 28040, Madrid, Spain
[e] Computational Archaeology (CoDArchLab), Institute of Archaeology, University of Cologne, Albertus-Magnus-Platz, D-50923, Cologne, Germany
[f] Unit associated to CSIC, Departamento de Paleobiología, Museo Nacional de Ciencias Naturales, C/ José Gutiérrez Abascal, 2, 28006, Madrid, Spain

ARTICLE INFO

Article history:
Received 25 November 2022
Received in revised form
21 February 2023
Accepted 28 February 2023
Available online 5 May 2023

Handling Editor: Danielle Schreve

Keywords:
Archaeostratigraphy
Machine learning
Lithic refitting
Palimpsest
Lower palaeolithic
Kill-butchering site
Pleistocene
Western Europe

ABSTRACT

Understanding the temporal resolution of archaeological deposits is a critical issue for drawing behavioural inferences. In the case of TD10.2 (Gran Dolina, Sierra de Atapuerca), this factor becomes essential in defining the mass communal bison hunting level and the different butchering events that took place at the sub-unit, which is characterised as a kill-butchering site. Traditionally, the dissection of events within an assemblage is performed by visual archaeostratigraphic techniques. This method, however, can be challenging in high-density sites without marked sterile gaps between levels. In this study, we present a combination of archaeostratigraphic techniques, supervised machine learning, and lithic refits applied to TD10.2. This integration of techniques offers a more automated and time-efficient archaeostratigraphic analysis, supports a more quantitative strand of evidence, and enables final verification using refits, even though it still requires prior visual archaeostratigraphic processing to set up qualitative data. Results have allowed for the definition of three distinct levels within the sub-unit along the entire excavation surface, highlighting the potential of these methods. Moreover, this approach facilitates the accurate delineation of level boundaries in the bison bone bed level, assessing its high spatiotemporal resolution, and identifying a minimum of two seasonal communal hunting events. This result reinforces previous interpretations while also providing new insights into the subsistence and behavioural strategies of the hominins that occupied the cavity.

© 2023 The Authors. Published by Elsevier Ltd. This is an open access article under the CC BY-NC-ND license (http://creativecommons.org/licenses/by-nc-nd/4.0/).

1. Introduction

The limited definition of the temporal readability of the archaeological record, led to the consideration of many deposits as palimpsests (Bailey, 2007; Binford, 1981a; Galanidou, 2000; Lucas, 2012). Archaeological deposits result from the interaction and overlapping of anthropic and natural phenomena that introduce, rework, disturb, and remove materials over different time spans, and at diverse temporal and spatial scales (Bailey, 1983; Butzer, 1982; Foley, 1981; LaMotta and Schiffer, 1999; Schiffer, 1987, 1983; 1972; Stein, 2001). The recurrence of activities, agents, and effects, generally produces the interstratification of materials belonging to different events in the same space and in a single analytical unit, giving rise to palimpsests (Villa, 1982; Bailey, 2007; Sullivan, 2008; Malinsky-Buller et al., 2011; Henry, 2012; Lucas, 2012). This issue is especially relevant for caves, attractive sights in the landscape where the recurrence of occupations in a physically constrained space, combined with habitually low sedimentation rates, which often results in palimpsests of coarse-grain resolution (Bailey and Galanidou, 2009).

In stratified deposits, archaeological assemblages are conventionally defined through geological criteria, with geological timescales exponentially longer than archaeological times (Adler et al.,

* Corresponding author. Universitat Rovira i Virgili (URV), Departament d'Història i Història de l'Art, Avinguda de Catalunya 35, 43002, Tarragona, Spain.
E-mail addresses: andion.arteaga@gmail.com, aarteaga@iphes.cat (A. Arteaga-Brieba).

https://doi.org/10.1016/j.quascirev.2023.108033
0277-3791/© 2023 The Authors. Published by Elsevier Ltd. This is an open access article under the CC BY-NC-ND license (http://creativecommons.org/licenses/by-nc-nd/4.0/).

2013; Stern, 1994). Nevertheless, although geological units provide important contextual information (e.g., palaeoclimatic conditions), their conformation varies independently of past behaviour (Mcpherron et al., 2005), and hence cannot be assimilated to cultural units. The discrepancies between the time-scales of geological and behavioural events imply that, through acritical aprioristic assumptions, archaeological materials found in a lithologically and sedimentologically defined archaeological unit, could be perceived as the result of a single occupation. This leads to many events being studied as contemporary activities, carried out at the same time and by the same group of individuals. The implicit idea that artefacts within the same unit are synchronic, supports the misleading illusion that assemblages represent a simple accumulation of contemporary decisions and actions. This contributes to the homogenisation of both the behavioural variability of humans and the different scales of analysis (Binford, 1981a; Dibble et al., 2017; Romagnoli et al., 2018).

In recent years, estimating the time resolution of an archaeological assemblage has become a critical issue in the archaeological discipline, leading to the formulation of a comprehensive theoretical framework around time-perspectivism phenomena and the archaeology of time (Bailey, 1981; Gowlett, 1997; Harding, 2005; Holdaway and Wandsnider, 2008; Lucas, 2012 and references therein). This time-averaged perspective (Stern, 2008, 1994), provided by the superimposition of multiple occupations in a single area, has traditionally been considered a drawback, claiming that the lack of discrete occupation episodes does not allow reliable spatial or behavioural inferences to be made. From this standpoint, archaeological endeavours have pursued the search for well-preserved deposits as a faithful depiction of prehistoric activities, delving into snapshots and high-resolution sites that approach the archaeological time to the ethnographical one as a baseline for interpretative analogies of the archaeological record (Bamforth et al., 2005; Machado et al., 2013; Pettitt, 1997; Schiffer, 1985; Smith, 1992; Vaquero, 2008).

Nevertheless, in a virtually dichotomous sense, some authors have also stressed the pitfalls of disentangling assemblages into minimal episodes where generalisations about prehistoric behaviour cannot be sustained (Bailey, 2007, 1983). If confronted with the epistemological meaning of the archaeological discipline as a historical science, concerned about time processes (Smith, 1992), then the synchronic scale of ethnographic time cannot provide reliable explanatory observations for large-scale evolutionary shifts (Dunnell, 1982; Kuhn and Clark, 2015; Smith, 1992; Vaquero et al., 2012).

From this perspective, several authors refer to the potential of time-averaged deposits, or palimpsests, for bringing visibility to the sites. This approach filters short-term noise, and provides broader information about long-term processes, complex interactions and adaptations, behavioural dynamics, or technological, ecological, and social trends, that may not be visible at an ethnographic scale of analysis (Bailey, 2007; Bailey and Galanidou, 2009; Kowalewski, 1996; Olszewski, 1999; Perreault, 2019; Reeves et al., 2019; Wandsnider, 2008).

Regardless of the nature of the deposit, understanding the temporal and spatial scale of the archaeological record becomes an essential premise to discern the degree of bias in an assemblage. This can additionally be used to address perspicuous research questions and develop suitable techniques and units of analysis (Bailey, 2007; Lyman, 2003; Sullivan, 2008). It is therefore fundamental to recognise palimpsests in terms of different events and distinct diachronic sequences, so as to reconstruct occupational patterns properly, and trace the subsistence strategies and eco-social behavioural models of the different hominin groups (Machado et al., 2015; Mallol and Hernández, 2016; Martínez-Moreno et al., 2016).

As pointed out by Romagnoli et al. (2018), the ability to craft a comprehensive narrative is still a challenge, especially when integrating the complexity of different temporal scales. This is applicable from the search for individual events, discrete episodes, and occupation floors, to the broader trends and evolutionary explanations afforded by long-term processes.

Unravelling the temporal idiosyncrasy and the contemporaneity of archaeological evidence has traditionally been the subject of archaeostratigraphical practice. Archaeostratigraphy focuses on the vertical dimension of sedimentary sequences, establishing minimum temporal analytical units within cultural deposits. This discipline pursues the identification of diachronic occupations and synchronic relationships among the different archaeological remains. Through this, analysts attempt to reconstruct individual episodes of activity, unearth subjacent formation processes and post-depositional disturbances, while providing a deeper understanding and resolution for the site. (Canals et al., 2003; Obregón Labrador, 2012; Sánchez-Romero et al., 2017; Sañudo et al., 2012).

This approach can be further enhanced by a greater variety of interdisciplinary proxies such as; micromammals distribution (Giusti and Arzarello, 2016), the occurrence of medium to large-size carnivores (Sañudo et al., 2016), taphonomic alterations (Discamps et al., 2019; Yravedra et al., 2016), and spatial analyses (Marín et al., 2019; Reeves et al., 2019; Romagnoli and Vaquero, 2016). Likewise, high-resolution techniques are also of interest, such as soil micromorphology (Leierer et al., 2019; Mallol et al., 2013; Vallverdú and Courty, 2012), charcoal examination (Mas et al., 2021; Vidal-Matutano, 2017), archaeomagnetism (Carrancho et al., 2016), tooth microwear analysis, or intra-tooth isotopic profiles (Julien et al., 2015; Rivals et al., 2009a, 2009b), among others.

The contribution of lithic and faunal refits is also particularly important to archaeostratigraphy. Refits sheds light on the archaeological record's time variable and event scale. The links between remains introduce punctual moments and discrete technical events while, at the same time, provide dynamic to the static nature of the archaeological record (Gowlett, 1997, p. 163; Romagnoli and Vaquero, 2019). The analysis of bone or artefact linkages additionally supports the assessment of the integrity of an assemblage, reinforces site formation reconstruction and taphonomic processes, underlies the comprehension of diachronic and synchronic relationships, corroborates archaeostratigraphic observations, and contributes to estimating the potential assemblage time span (Ashton, 2004; Bargalló et al., 2016; Bordes, 2003, de la Torre et al., 2012; Deschamps and Zilhão, 2018; Fernández-Laso et al., 2020; Hofman, 1986; López-Ortega et al., 2019; Machado et al., 2019; Morrow, 1996; Rosell et al., 2012; Sumner and Kuman, 2014; Vaquero et al., 2017, 2012; Villa, 1982).

Nowadays, the archaeostratigraphic perspective is widespread and incorporated into most academic research. Nevertheless, despite the contribution of the methods mentioned above, or the occasional inclusion of more advanced statistical techniques (e.g., Anderson and Burke, 2008; Ngoloyi et al., 2020), archaeostratigraphic practice is essentially a qualitative method, highly conditioned by the techniques used to document the archaeological record. Likewise, human induced factors, such as the observer's training and experience, are also important, while the nature of the deposit itself is also likely to condition subsequent interpretations. This is particularly clear in large open surface excavations with densely clustered materials, no anthropogenic structures, and blurred stratigraphic boundaries, where the dissection of palimpsests is rather limited and reliant on the observer's subjective criteria.

Recently, a new proposal has been published applying unsupervised and supervised machine learning (ML) algorithms to

identify palaeontological fossiliferous levels (Martín-Perea et al., 2020). ML algorithms are a subset of Artificially Intelligent (AI) algorithms, based on the construction of mathematical functions to perform specific tasks. Several types of algorithms exist under different "learning" paradigms, all of which have distinct advantages or disadvantages according to the task at hand. In ML, the concept of "learning" is based on the use of well-known data (training set) to train the algorithm over a series of iterations, using trial and error to reduce the number and severity of mistakes made (Bishop, 2006; Goodfellow et al., 2016). Throughout this process, algorithms adjust their own internal parameters, thus "learning" from this data. Once trained, algorithms are provided with new data (test set) to be tested and evaluated. When exposed to more data over time, these methods improve and can produce models with high predictive accuracy from almost any data type.

In the last decade, these quantitative methods have increasingly been introduced into the archaeological discipline (Bickler, 2021), with special emphasis on several areas of taphonomic research (Arriaza and Domínguez-Rodrigo, 2016; Cifuentes-Alcobendas and Domínguez-Rodrigo, 2019; Courtenay et al., 2021, 2020; Domínguez-Rodrigo and Baquedano, 2018; Moclán et al., 2019), lithic technology and experimental replication (Archer et al., 2021; Bustos-Pérez and Baena, 2021; González-Molina et al., 2020; Grove and Blinkhorn, 2020; Nash and Prewitt, 2016; Orellana Figueroa et al., 2021), rock art identification (Jalandoni et al., 2022), as well as geological and archaeological surveys (Elliot et al., 2021; Orengo et al., 2020; Thabeng et al., 2019).

These studies highlight the significant improvement in the accuracy and reliability of the results compared to other statistical techniques or more conventional procedures. ML algorithms are thus highly efficient at processing large and complex multidimensional datasets and provide a more robust and empirical approach to processing such data (Cobo-Sánchez, 2020; Domínguez-Rodrigo, 2019).

Based on these renewed approaches, this study presents, for the first time, the application of supervised ML algorithms for the archaeostratigraphic study of the archaeological cave deposit of the Gran Dolina TD10.2 sub-unit (Atapuerca), in combination with conventional archaeostratigraphic methods and information derived from lithic refits. This sub-unit provided evidence for a monospecific bison kill-butchering site, interpreted as the earliest evidence of mass communal hunting (see further details below) (Rodríguez-Hidalgo et al., 2017). Due to the relevant implications of this assemblage, which reflects high organisational capabilities, sophisticated subsistence strategies, and social cooperation, it has been considered essential to discern its spatio-temporal definition and estimate its potential to infer behavioural trends.

The aims of this research are; a) to define the different formation phases of the sub-unit TD10.2; b) to evaluate the applicability and effectiveness of ML-based approaches for dissecting sedimentary units; and c) to explore whether the archaeological layer formed by the bison bone bed (TD10.2-BB) can be disentangled into smaller analytical units to gain insight into its temporal and functional significance. From this perspective, we aim to provide a better time and spatial resolution framework for the study of human activities and occupational patterns carried out in Gran Dolina TD10.2.

2. The litostratigraphic sub-unit TD10.2

The archaeo-palaeontological site of Gran Dolina is part of the intermediate karst level of the Sierra de Atapuerca, Burgos (Spain), being the northernmost site of the Trinchera del Ferrocarril archaeological complex. The cavity presents a keyhole section morphology, infilled with 25 m of autochthonous (units TD1-2) and allochthonous sediments (TD3/4-TD11) (Campaña et al., 2017; Duval et al., 2022; Ortega et al., 2013), where originally eleven lithostratigraphic units were identified, from bottom to top (TD1-TD11) (Gil et al., 1987; Parés and Pérez-González, 1999; Pérez-González et al., 2001) and subsequently revised (Campaña et al., 2017; Parés et al., 2018; Rodríguez et al., 2011; Vallverdú, 2017) (Fig. 1).

TD10 is the youngest archaeo-palaeontological lithostratigraphic unit, with ESR-U/Th, TL-IRSL, and ESR OB dates that situate the deposits between MIS11 and MIS8 (Berger et al., 2008; Falguères et al., 1999; Moreno et al., 2015). It is divided into four lithostratigraphic sub-units, TD10.1 to TD10.4, from top to bottom respectively. Sedimentary processes are mainly exokarstic in origin. The dominant mechanism is the gravitational fall of sloping debris at the cave entrance (falling blocks, debris flows, and furrow flows); however, small inputs of secondary lateral entries of material have also been documented (Campaña, 2018; Campaña et al., 2017; Mallol and Carbonell, 2008; Vallverdú, 2013). These breccia-filling sedimentary processes form ordered debris deposits.

This 3 m-thick succession has recently been concluded through an extensive excavation over approximately 95 m^2 (Fig. 2). It reflects a relatively continuous succession of hominin occupations, technologically evolving from the Acheulean (TD10.4 and TD10.3), to assemblages showing certain transitional features pointing to an early Mode 3 technology in TD10.2 (ongoing study), and TD10.1 (Carbonell et al., 2001; Menéndez Granda, 2009; Terradillos Bernal and Díez Fernández, 2012; Ollé et al., 2013, de Lombera-Hermida et al., 2020).

Despite some disagreements between the different proxies employed, no significant climatic changes have been detected. The main environmental reconstructions thus point to climates similar to interglacial conditions, with occupations of TD10 occurring in a rather temperate period (Blain et al., 2009; Cuenca-Bescós et al., 2005; Rodríguez et al., 2011).

Formation processes and occupational patterns also vary throughout the sequence. TD10.1 is divided into two major archaeological deposits (Fig. 2a). The top of the sequence (Upper TD10.1) reveals a succession of logistical and short-term occupations (Saladié et al., 2018). The bottom of the sub-unit (TD10.1-BB) exhibits a high-density bone bed of about 10 cm-thick, interpreted as a long-term residential camp (de Lombera-Hermida et al., 2020; López-Ortega et al., 2017; Márquez et al., 2001; Ollé et al., 2013; Pedergnana and Ollé, 2020; Rodríguez-Hidalgo et al., 2015). Other studies have also focused on the intermediate part of the sub-unit, tracing punctual activities or occupations that do not always correlate with comprehensive archaeostratigraphic entities (Blasco et al., 2013; Rosell, 2002).

Conversely, the current ongoing analysis of sub-units TD10.3 and TD10.4 suggest sporadic occupations of low intensity and relatively reduced anthropogenic impact.

Sub-unit TD10.2, the focus of this study, is approximately 1 m-thick. Current available geochronological studies (Fig. 1c) have provided two ESR/U-series dates (418 ± 63 ka and 337 ± 51 ka) on ungulate teeth (Falguères et al., 2001, 1999), for the upper part of the sub-unit, and ESR dates on quartz grains (375 ± 37 ka and 378 ± 10 ka) for the medium and basal portions (Moreno et al., 2015). OSL dating, however, has reported a slightly discordant mean date of 244 ± 26 ka for the deposit (Berger et al., 2008) (from one sample at the top and two at the bottom), which substantially rejuvenates the results provided by ESR. The inconsistencies and uncertainty about the established dates may be related to the different radiometric methods applied, since ESR/U–Th tends to provide older dates than luminescence (Rodríguez et al., 2011). A new series of OSL dating is in progress (single grain TT-OSL and pIR-IR, Arnold et al., 2015), which will hopefully help clarify these discrepancies.

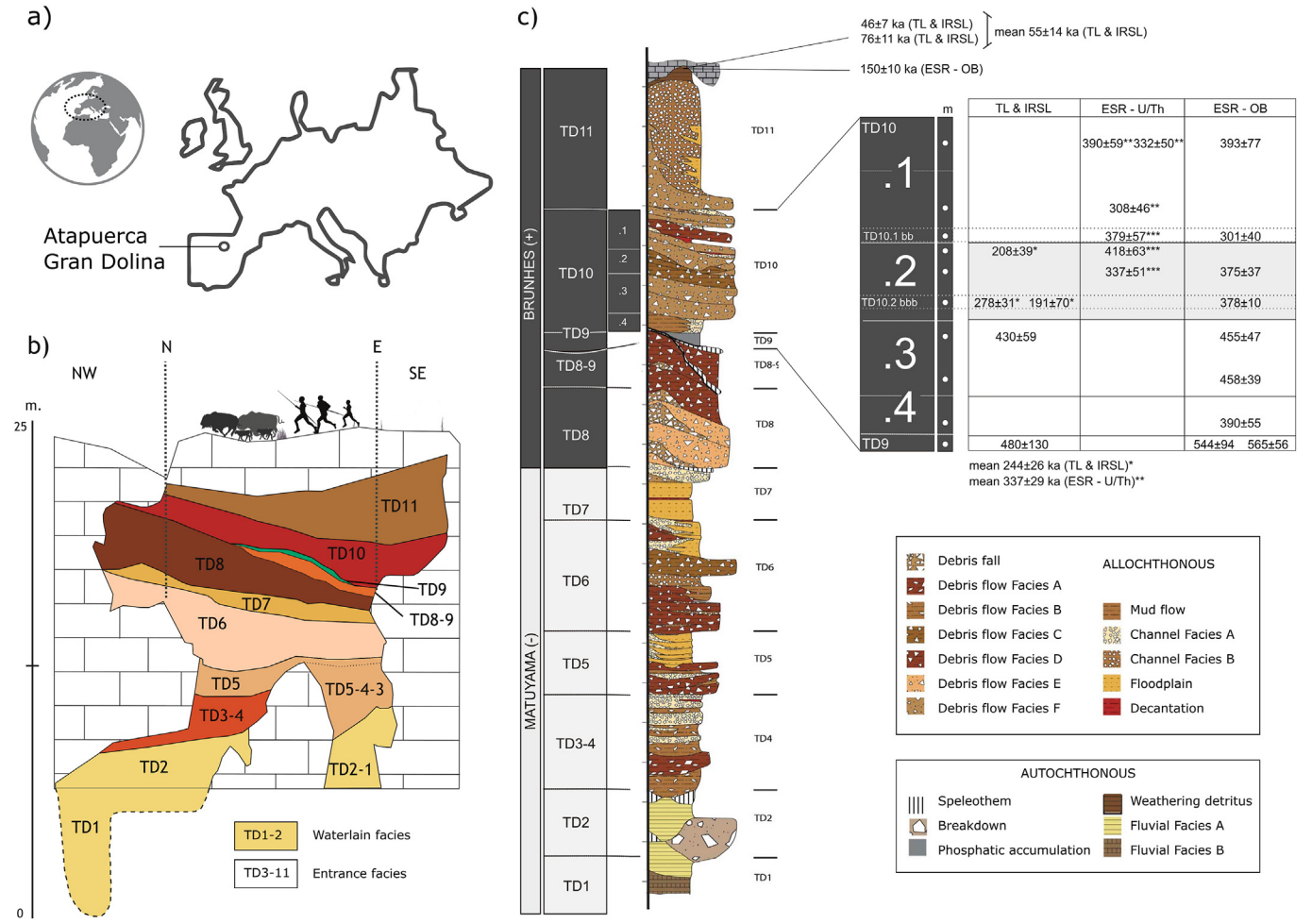

Fig. 1. a) Location of Gran Dolina and Sierra de Atapuerca, in the North of the Iberian Peninsula; b) Gran Dolina's paleomorphology from the railway trench (south archaeological section) and main lithostratigraphic units; c) Synthetic sedimentary facies column of Gran Dolina site and location of available dates for TD10 (Berger et al., 2008; Falguères et al., 1999; Moreno et al., 2015). (Figures modified from Campaña et al., 2017, p. 79; Duval et al., 2022, p. 2; Rodríguez-Hidalgo et al., 2017, p. 91).

The TD10.2 deposit consists of a reddish-brown mud matrix with heterogeneous limestone gravels and blocks derived from the structural degradation of the cave. It presents a texture with a polymodal composition (granules, fine gravels, medium gravels, and microgranular massive muds) and a homogeneous appearance that blurs the recognition and mapping of possible stratigraphic discontinuities (Vallverdú, 2013). Accordingly, the archaeological excavation has highlighted the homogeneity of the sedimentary matrix, with no significant macroscopical changes in colour, texture, or structure, although a progressive decrease of gravels towards the bottom in favour of an increment of clays has been observed (Campaña, 2018).

Despite the aforementioned sedimentological uniformity, fieldwork revealed an archaeostratigraphic horizon with a noteworthy concentration of lithic and faunal remains at the bottom of the sub-unit. The previous archaeostratigraphic analysis (Rodríguez-Hidalgo, 2015; Rodríguez-Hidalgo et al., 2017) defined this accumulation as a specific archaeolevel within the sub-unit, called bison bone bed (TD10.2-BB). This horizon, however, could not be confidently traced over the entire excavation surface, as it decreased in entity at its periphery. TD10.2-BB was, therefore, restricted to the northern and northwestern area of the excavation surface (approx. 55 m^2), until further in-depth archaeostratigraphic study of the entire excavation area (Fig. 2b).

Additionally, during the 2011 and 2012 field seasons, slight compositional changes were noticed at the bottom of the bone bed. These included a decrease in the density of remains, a gradual transition to smaller and unidentifiable bones, the increased carnivore occurrence and taxa variability, occasional appearance of large lithic formats, a greater weight of sandstones and quartzite in the overall composition, and minor shifts in sediment colouration and compaction. These factors led to the decision to give this record its own entity and designate it as archaeolevel TD10.2.2.

The information supplied by the zooarchaeological study of 24,216 faunal remains from the bison bone bed archaeolevel reveals a highly monospecific assemblage dominated by *Bison* sp., with at least 60 individuals. The intensive and systematic processing of carcasses testifies early and primary access of hominins. Scavenging by medium-sized and large carnivores is registered after hominins abandoned the area. The dominance of axial bones, selective transport of the high-yield elements (limbs) outside the cave, seasonality death patterns, and catastrophic mortality profiles (closely resembling a living population structure, see Rodríguez-Hidalgo et al., 2017, p. 97), point to mass predation as the hunting strategy. The available evidence supports the interpretation of the site as a monospecific bison kill-butchering site (Rodríguez-Hidalgo, 2016, 2015; Rodríguez-Hidalgo et al., 2017, 2016).

Preliminary technological analysis of the overall TD10.2 lithic

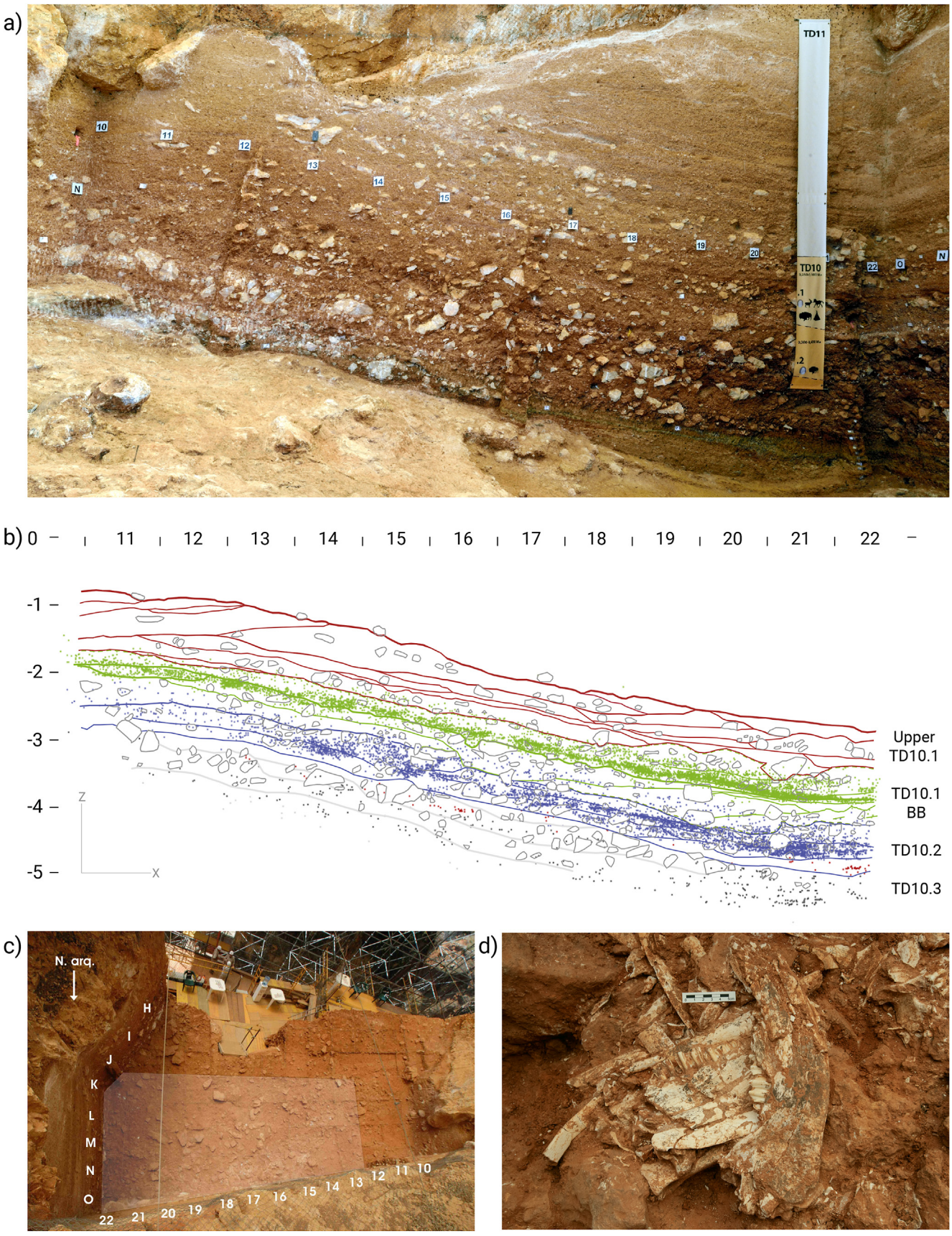

Fig. 2. a) Profile picture of the TD10 sequence; b) Transverse cross-section (20 cm-thick) of TD10.1, TD10.2 and the upper part of TD10.3 projected in a stratigraphic drawing of the northern section of TD10. Figure modified from Saladié et al. (2018); stratigraphy representation done by Josep Valverdú; c) Excavation area of Gran Dolina site, field season 2009. The bleached polygon indicates the area analysed by Rodríguez-Hidalgo et al. (2015, 2017); d) Detail of bison remains from TD10.2-BB, lying on a barely sterile sediment. Pictures by Andreu Ollé.

assemblage indicates intense knapping activities at the site, with the presence of complete reduction sequences, and an over-representation of small flake products. Shaping processes are focused on the production of a notable variability of small tools on flake while, on the contrary, the occurrence of large cutting tools (LCT) is very limited. Knapping strategies are diversified, but the centripetal reduction is predominant and is generally carried out through bifacial volumetric strategies (Arteaga-Brieba et al., 2020; Ollé et al., 2013). Preliminary use-wear results coincide with zooarchaeological and taphonomic data, which point to mainly butchery-related activities, while the working of bone, wood and hide have also been identified (Asryan et al., 2022, 2021; Rodríguez-Hidalgo et al., 2017).

Raw material procurement is local and reveals an extremely high specialisation in Neogene and Cretaceous chert, not documented in other sites of the Sierra de Atapuerca complex. Materials from the nearby terraces (quartzite, sandstone, and quartz) are scarcely represented and mainly related to LCT and hammerstones (García-Antón, 2016; Ollé et al., 2013; Soto et al., 2021).

3. Materials and methods

As part of the fieldwork protocol at Gran Dolina, all lithic artefacts, identifiable faunal remains (regardless of size, yet excluding micromammals and mesovertebrates such as leporids and small birds), and any bone greater than 2 cm have been registered on horizontal and vertical planes through three-dimensional Cartesian coordinates, established with a *3COORDsystem* (Canals et al., 2008), and a total station theodolite. Limestone blocks larger than 10 cm have been recorded by taking an upper and lower central point. The entire perimeter of limestone blocks bigger than 50 cm was also digitised. The use of a total station records the position of each data point with an accuracy to the closest millimetre, thus enabling the subsequent 3D virtual reconstruction of the archaeological deposit (Dibble, 1987; Mcpherron et al., 2005).

Archaeostratigraphic analyses were conducted by considering all faunal and lithic data. Materials recovered through sieving sediments were excluded due to the inaccuracy of their coordinates. Small blocks have also been omitted owing to their overwhelming presence, very homogeneous throughout the sequence, a circumstance that obscures the identification of discrete layers. Blocks larger than 50 cm have been accounted for in the projections since large block falls can be considered as part of the (natural) architecture of the occupational surfaces of the cave. They may also be indicative of cavity abandonment phases and a potential source of vertical distortion, as well as material vacuum gaps (Mora Torcal et al., 2020, p. 46).

Instead of focusing only on sub-unit TD10.2, the information provided by previous archaeostratigraphic studies concerning lower TD10.1 (de Lombera-Hermida et al., 2020; Obregón Labrador, 2012), TD10.2 (Rodríguez-Hidalgo et al., 2017), and ongoing analysis for the top of TD10.3 (Mosquera et al. in prep), was also used as a frame of reference for the current analysis. This approach facilitates a better definition of the upper and lower boundaries of TD10.2, while checking for possible sub-unit ascription inconsistencies during archaeological fieldwork. Overall, 158,831 coordinate points have been considered for this study (43.79% corresponds to lower TD10.1; 45.85% to TD10.2; 2.72% to TD10.2.2; and 7.64% to the upper part of TD10.3; according to ascriptions made in field seasons; see Table A.1).

3.1. Visual identification of archaeostratigraphic levels

The entire surface of the assemblage (bottom of TD10.1, TD10.2 and upper part of TD10.3) has been dissected into adjacent cross-sections of 20 cm thickness on its transversal (east-west) and longitudinal (north-south) axes. Some diagonal cross-sections have also been made, following the direction of the main slope.

A visual test of multiple thicknesses (10, 20, 40, 50 cm and 1 m) led to this thickness choice as it contains enough density of materials, allowing for the exploration of spatial distributions and the detection of different sublevels. Furthermore, this thickness avoids overlapping and obliteration effects caused by the dip and strike of the archaeological horizons, thus preventing thin sterile hiatuses from being obscured.

Cross-sections have been created by the Geographic Information System (GIS) ArcGIS® software (v.10.8.1) and have been processed and displayed with its software extensions ArcMap (Gallotti et al., 2011, p. 378) and ArcScene. The latter allows for the 3D visualisation of data, enabling the user to rotate and adjust each projection according to the dip and topography of each section (Roy Sunyer, 2016).

All the projections have been analysed sequentially, following the main stratigraphic criteria proposed by Canals (Canals et al., 2003; Canals and Galobart, 2003). First, the continuous vacuum space along the surface was used as the primary source of evidence to establish the boundary between two archaeological entities. These voids, or spaces of low archaeological density, represent sterile hiatuses, moments of sedimentation during which there is no input of archaeo-palaeontological material, or its density is drastically lower compared to the upper or underlying level. Next, the slope or surface of each deposit is identified by considering the base of the first elements deposited in the level. Their outline allows for the reconstruction of the original palaeosurface, revealing its slope and the direction of sedimentation. Finally, vertical void spaces can be used as potential indicators of block falls, bioturbations, small water channels, or runoffs partially eroding the assemblage (Obregón Labrador, 2012).

We have observed the vertical distribution of various categorical variables, including the type of remains (fauna, lithic), size, presence of carnivores, raw materials, taxa, as well as limestone blocks larger than 50 cm. When possible, seasonality-related data (Rodríguez-Hidalgo et al., 2016) have also been incorporated into visualisations. In Fig. 3, some examples are illustrated.

The verification of the stratigraphic assignment has been carried out by establishing control points at the intersections between the transversal and longitudinal projections. A sequential analysis has been employed to guarantee coherence and consistency in the level assignment, testing each section against the prior and the subsequent ones. In those circumstances where there is a discrepancy between the level designated in transversal and longitudinal projections, a cautious stance has been adopted, and no level has been preliminarily assigned to the specific point, keeping them as indeterminable.

3.2. Supervised machine learning

Visualising vertical cross-sections across the site allows for the classification of different archaeological levels within TD10.2. Nevertheless, issues regarding the density of points and the complexity of depositional processes hindered this procedure for several data points. In order to overcome this, two different supervised ML classification algorithms were implemented to assign these pieces to a level, following the methodological proposals of Martín-Perea et al. (2020). These include:

- Support Vector Machines (SVM): Algorithm developed in the 1990s, based on the classification of points in a sample by creating optimal hyperplanes used as discriminant decision surfaces. Hyperplanes are constructed and learned from the

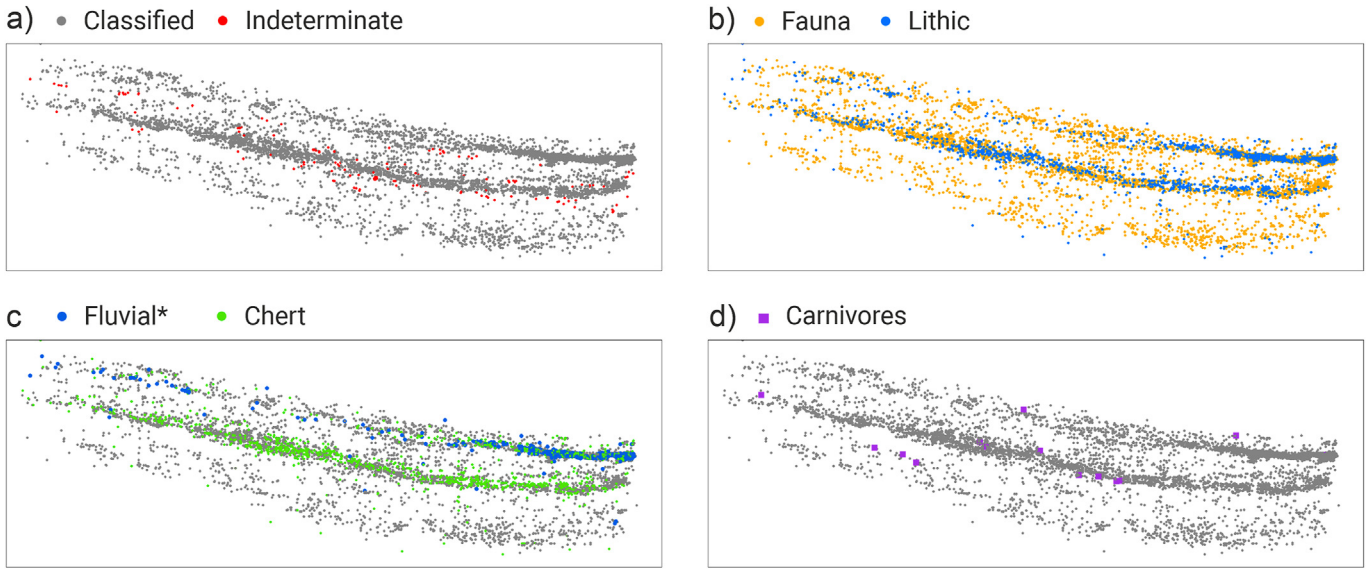

Fig. 3. Process of archaeostratigraphic classification in the M-line cross-section (Y coord. 1280–1300 cm): a) In grey, materials with levels assigned according to classical archaeostratigraphic techniques; in red, indeterminate material to be classified through ML algorithms; b) Projection of faunal (yellow) and lithic (blue) remains; c) Projection according to raw materials. In green, Neogene and Cretaceous chert, in blue (*), materials from the fluvial terraces in the surroundings of Sierra de Atapuerca (quartzite, sandstone, and quartz), grey colour indicates faunal remains; d) Presence of carnivores (purple).

training data using an optimisation procedure that maximises hyperplane margins and thus reduces overfitting. In non-linear datasets, data separation is achieved by applying kernel functions, which allow additional dimensions to be added to the workspace (Cortes and Vapnik, 1995). SVMs are highly complex and powerful algorithms that work well for both classification and regression tasks. SVMs were implemented in the R (v.4.0.4) programming language via the "e1071" (v.1.7) and "caret" (v.6.0) libraries (Kuhn, 2020; Meyer et al., 2021).

- Random Forest (RF): This algorithm is based on a decision tree classification that uses random samples selected by bootstrap aggregation within the dataset to build an independent decision tree for each sample. Multiple decision trees are generated on trained datasets, and the results are subsequently averaged to obtain a single robust classification model. The unestimated observation in the performed trees (out-of-bag) is used for automatic validation of the model (Breiman, 2001). RFs were implemented via the "caret" (v.6.0) library (Kuhn, 2020).

Both algorithms were trained using a cross-validation approach ($k = 10$), with a 70:30% train-test split (70% of the data are used for training while the remaining 30% is reserved for evaluation).

Algorithms were trained gradually across the assemblage, dividing the site into a series of profiles, training the algorithms on these profiles, and then using algorithms to propagate level boundaries across the whole assemblage. Algorithms were retrained on each section until the entire surface had been processed (Table A.2). This stepwise process enhances the classification strength and robustness of algorithms, allowing both SVMs and RFs to adapt their decision boundaries to the different topographical changes across the archaeological levels.

One metre thick sections were chosen for this step as no significant differences in the results have been perceived with 20 cm thick sections. This option also improves the computational cost of using this system on larger sites.

Standardised ML protocols have been applied to evaluate the different models. This includes calculating accuracy, sensitivity and specificity metrics when using algorithms to classify the test sets. Accuracy refers to the total classified data among the total data given for training. This score sometimes does not reflect model performance when data are imbalanced, therefore must be accompanied by other measurements, such as Sensitivity (the true positive rate), Specificity (the true negative rate) and Balanced Accuracy values (the arithmetic mean between Sensitivity and Specificity). Each of these indices is derived from confusion matrix results, and is particularly useful for assessing each model's efficiency. The Kappa (κ) statistic can also be used to test inter-rater reliability. κ evaluates the probability that predicted labels will coincide with the original labels. κ is normally interpreted considering values above 0.5 to present moderate agreement, values between 0.6 and 0.8 to present substantial agreement, and 0.8 to 0.99 presenting near perfect agreement (Landis and Koch, 1977).

The final classification of the archaeological assemblage was made by evaluating results produced by the two models, establishing 80% as the probability threshold to consider a fossil confidently associated with a level (Martín-Perea et al., 2020). Archaeological remains assigned to a level with less than 80% confidence are thus classed as indeterminable. In cases where SVM and RF algorithms disagree on the level adscription, the model with the greatest confidence in the prediction is chosen.

The root of the Mean Squared Error (RMSE) and the median confidence were calculated for each model to assess the quality of the overall system when combining SVMs and RFs, as well as a means of assessing the quality of the final profiles. Additionally, κ statistics were once again calculated to assess the efficiency of the artificially intelligent system. This was performed by evaluating the inter-observer agreement between SVMs and RFs (Cohen, 1960).

3.3. Lithic refitting

A systematic refitting program has been carried out entailing the lithic remains from the whole sub-unit TD10.2, recovered in the field seasons from 2006 to 2013. 488 artefacts (4.34% of the assemblage) from previous seasons have been omitted from the study. The first step was to separate artefacts by raw materials,

where six different lithological groups were identified; Neogene and Cretaceous chert, quartzite, sandstone, quartz, and limestone. In this process, hardly any raw material units (Roebroeks, 1988) have been identified, except in particular circumstances, due to the presence of a covering whitish patina over the entire surface of chert that obliterates any macroscopic differential features.

Apart from complete *manuports* and hammerstones, all quartzite, quartz, and sandstone items, have been considered. This was performed irrelatively, as their representation in the assemblage is scarce. Objects smaller than 15 mm have been excluded for the case of chert. All poorly preserved materials have also been discarded for analyses. This affects certain sandstones with a high degree of erosion due to a loss of surface grain cohesion, as well as the particular case of Neogene chert, which is notably altered by chemical weathering, even involving the disintegration of its internal structure (Font et al., 2010; Ollé et al., 2013). After this initial screening, circa 3.500 artefacts have been considered as potential artefacts that can be refitted.

The refitting analysis is integrated into a broader and more exhaustive study focused on its technological features and spatial distribution (preliminary results in Arteaga-Brieba et al., 2021). In this study, only information with direct archaeostratigraphic applicability is discussed. For this purpose, all lithic connections have been classified according to their link type as refit or conjoin (Cziesla, 1990; Sisk and Shea, 2008), and have been projected individually and within their refit group. Firstly, the archaeostratigraphic positions of refitted artefacts were classified using ML algorithms, independently of their condition as refits and their archaeological significance, while using them as an independent strand of evidence to evaluate the stratigraphic integrity of TD10.2. Afterwards, each piece's previous classification was checked and verified with 3D cross-sections.

4. Results

In this section, we will show how the combination of the in-depth visualisation of the 3D cross-sections and artificial classification methods has led to the identification of three different levels across the entire surface within sub-unit TD10.2; Upper TD10.2 (top), TD10.2 bison bone bed (TD10.2-BB) and TD10.2.2 (bottom). The detailed examination of each fine-tuned projection has confirmed previous archaeostratigraphical studies, allowing the ascription of nearly all the archaeological remains, and has also helped in refining the boundaries of each level. Several groups of lithic refits have also corroborated the observations made in the field, alongside each of these archaeostratigraphic assessments.

4.1. Cross-section analysis

In the initial step, manual archaeostratigraphic subdivision allowed for the majority of remains to be assigned to a specific level (n = 152,734). 6097 items (3.84% of the sample), however, remained indeterminable due to their uncertain ascription. Most of these archaeological remains are located on the limits between the different levels observed in TD10.2. In these instances, the locations were separated for subsequent classification using supervised ML algorithms (Fig. 3a).

A decisive criterion for the manual archaeostratigraphic subdivision in TD10.2 is the evident change in density between the upper part and the underlying bison bone bed, with a noticeably higher material concentration (Figs. 4 and 5). The bone bed located at the base of TD10.1 (TD10.1-BB), usually delimits the lower boundary of the sub-unit, while beneath it, there is a more or less continuous scattering of materials across the entire excavation surface. This phenomenon terminates with the appearance of a second bone bed; the so-called bison bone bed. Two main aspects have reinforced this visual perception: the continued over-representation of bison remains in TD10.2-BB, as opposed to a slight increase of cervids and equids in Upper TD10.2, as well as the uneven distribution of raw materials in the different sublevels, with the overriding presence of chert in the bison bed (Fig. 3c). For the definition of level TD10.2.2, we have again considered the drastic drop in the density of materials, linked in large parts of the excavation to a thin sterile hiatus and the reappearance of non-chert raw material varieties.

The disposal of large limestone blocks has also played a significant role in delimiting these sublevels. The visualisation of each cross-section has enabled the discrimination between two main events of large block falls; one between Upper TD10.2 and TD10.2-BB, and a second event below the bison horizon. These large blocks cause ruptures in the continuous scattering of the remains across the surface, while their individualisation helps in the reconstruction of the cavity's original palaeotopography in the different occupational periods. Particularly relevant is the documentation of a block fall in the southeast area of the site, with great affectation to level TD10.2.2 (Fig. 5c).

Other variables observed, such as the presence of carnivores (Fig. 3d), or the size of the remains, seem to behave uniformly and have not proved useful for establishing discriminant criteria for each of the levels.

4.2. Fine-tuned classification with supervised ML

The application of ML algorithms for indeterminate materials has been able to classify 5595 (91.77%) of these remains (Table A.3). 502 (8.23%) specimens, however, were assigned to a level with less than 80% confidence, and thus remained indeterminable.

Results obtained from confusion matrices reveal accuracy and kappa values to be above 98% for both algorithms, reflecting a confident degree of classification. TD10.2.2 yields the lowest sensitivity values (SVM = 0.81; RF = 0.88) although, in all cases, the median of the balanced accuracy is higher than 90% (Table 1). Weaker scores for TD10.2.2 are explained by the lower number of components in this sublevel, compared to the rest of the dataset. The overall probability of level association reveals models to be ≈ 91.17% confident with each of their classifications. An in-depth analysis of confusion matrices reveals RF algorithms to be less sensitive to sample imbalance.

When comparing the performance of combining both algorithms in an artificially intelligent system, SVM and RF agreed on 83.34% of their classifications. SVM appears to be the most decisive algorithm 58.37% of the time when there is a disagreement. Cohen's κ calculation shows inter-rater reliability of 0.66, which indicates a substantial agreement (Landis and Koch, 1977). Although agreement-disagreement rates are not optimal, we can conclude that the combination of both algorithms still provides a powerful and robust method for automatic archaeostratigraphic classification, considering how the predicted probabilities of label association are still high (see further details in the discussion).

Owing to the particular circumstances of this study, the decision of applying AI algorithms was adopted once the visual assignment of levels was at a very advanced stage, so that the number of undetermined materials to be classified by ML is a very small percentage of the overall remains.

Considering this disjunctive, it was hypothesised whether the good performance of the algorithms is attributable to the substantial amount of information provided, and the threshold of prior information required to ensure reliable results. For this purpose, a single 1 m thick cross-section (line M) was examined and used to retrain the algorithms, randomly resampling from the training set

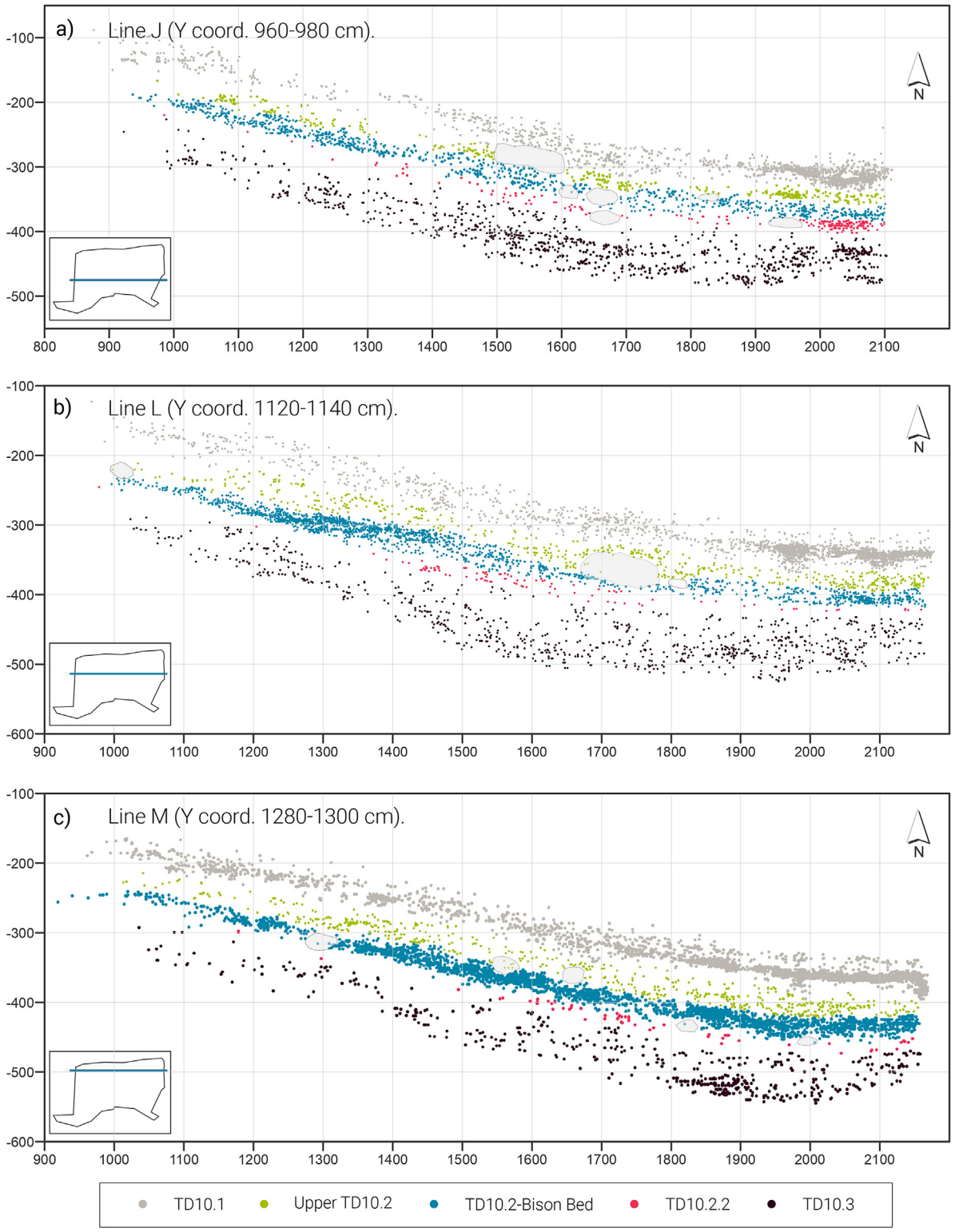

Fig. 4. Representative transversal (E–W) 20 cm thickness cross sections observed from the South profile of Gran Dolina; a) Line J (Y coord. 960–980 cm); b) Line L (Y coord. 1120–1140 cm); c) Line M (Y coord. 1280–1300 cm). The complete sequence of transversal cross sections can be found in Appendix C.

to use different percentages (1%, 5%, 10%, 20% … 90%) of information so as to classify the fossils from the test set.

Results yield kappa values above 0.8 in all training operations, providing a good performance of both algorithms even when only 1% of the overall data is employed as archaeostratigraphic information (Table 2). In all instances, RF trains more efficiently than SVM. This might be explained mainly on the basis that RF appears to be less conditioned by the sample imbalance phenomenon in the present case study. Sensitivity values show that RF manages to overcome the classification threshold of 0.8 from 10%,

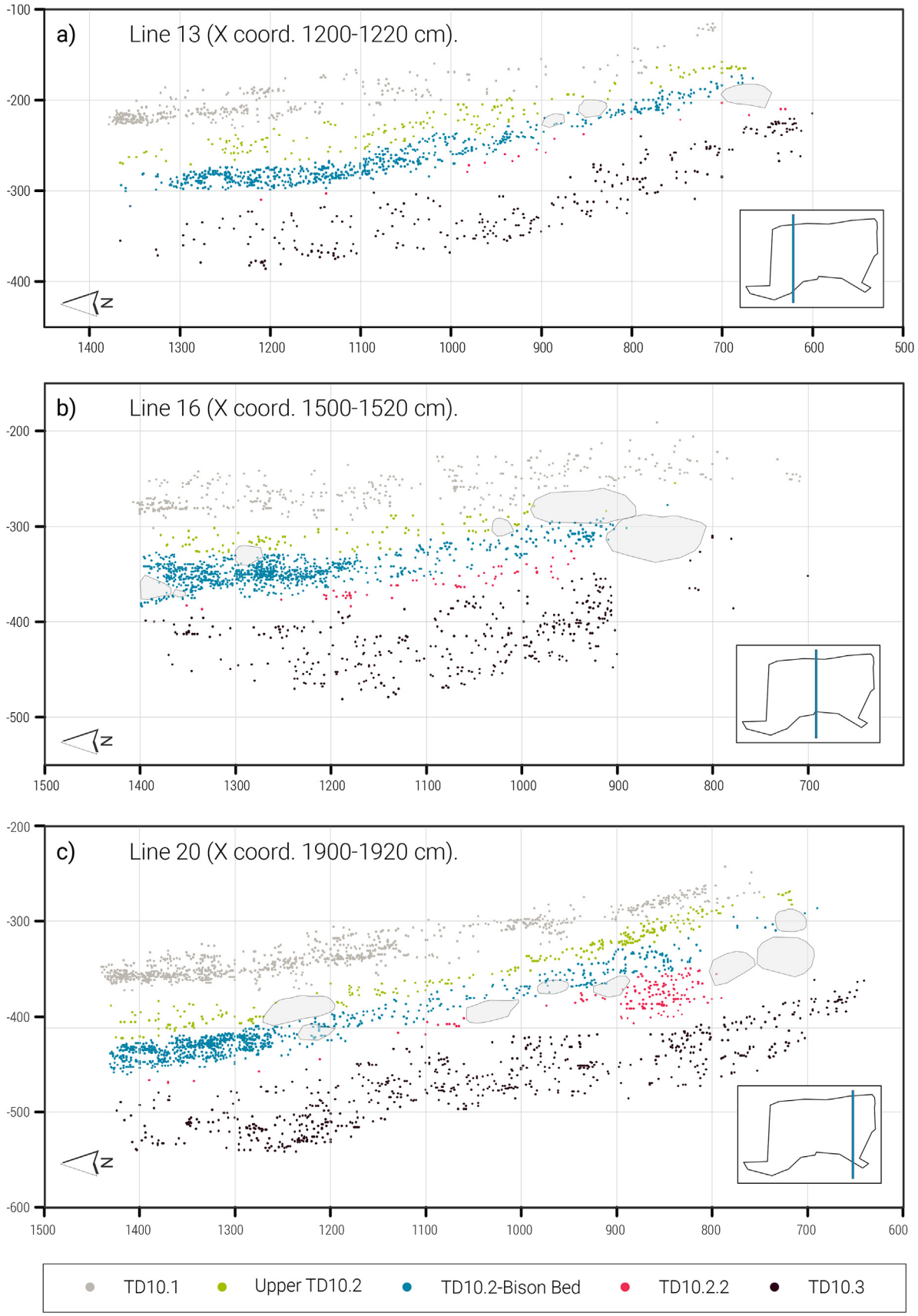

Fig. 5. Representative longitudinal (N–S) 20 cm thickness cross sections, observed from the West profile of Gran Dolina; a) Line 13 (X coord. 1200–1220 cm); b) Line 16 (X coord. 1500–1520 cm); c) Line 20 (X coord. 1900–1920 cm). The complete sequence of longitudinal cross sections can be found in Appendix C.

Table 1
Model performance for each of the ML algorithms when used to classify the test set. Summary (median) of parameter values for each ML algorithm. Extended version in Table A.4.

Algorithm	Accuracy	Kappa	Level	Sensitivity	Specificity	B. Accuracy
SVM	0.983	0.972	TD10.1	0.997	0.996	0.997
			Up. TD10.2	0.867	0.995	0.932
			TD10.2-BB	0.990	0.984	0.987
			TD10.2.2	0.810	0.999	0.904
			TD10.3	0.985	0.999	0.992
RF	0.991	0.986	TD10.1	0.999	0.998	0.998
			Up. TD10.2	0.949	0.998	0.973
			TD10.2-BB	0.996	0.993	0.995
			TD10.2.2	0.884	0.999	0.941
			TD10.3	0.990	0.999	0.995

while SVM does not overcome the problems derived from unequal simple size until 40% of the total information is given for training (see appendix B). Archaeostratigraphic observation of the different re-trainings does not reveal significant changes in level assignment.

Results indicate that only a rough prior manual classification is required to obtain robust classification with supervised ML techniques. This could be a substantial advantage, greatly reducing time investment in archaeostratigraphic processing.

4.3. Lithic refitting

The refit process has yielded 70 refit groups, entailing a total of 225 lithic artefacts. Cretaceous chert is the raw material with the highest number of lithic connections, some of which represent nearly complete exploitation processes. While Neogene chert dominates the assemblage, refits are far less common given the poor preservation of their surfaces and are mostly related to technological or post-depositional conjoins. Although only three refitting groups have been identified within quartzite, this raw material returns the highest refit success rate, displaying long reduction sequences. Sandstones and especially quartz are minority raw materials and yield limited results (Table 3).

The most represented knapping activity in the refit groups is the core exploitation for obtaining small flakes; however, shaping and maintenance activities have also been identified, verifying the existence of complete *chaîne opératoires* in the site.

The vertical distribution of refitted artefacts is largely aligned with the general slope of the assemblages, conforming to the palaeotopography. The archaeostratigraphical classification of the refits, by means of artificially intelligent algorithms and posterior cross-section verification, has enabled the assignment of each group to its corresponding archaeolevel (Table 4). In general, results from refitting are highly consistent with the identified horizons, with almost no migrations or vertical displacements detected within the elements of the same set (Fig. 6). Only two groups within TD10.2-BB present stratigraphic mismatches, with two single connections between adjacent levels.

The first is SC-01-TD10.2. The group consists of a Cretaceous chert set of nine elements, reflecting part of an orthogonal reduction strategy of a core. While eight elements (including the core) are found at the top of TD10.2-BB, a fragmented flake which refits directly to the core is located at the base of Upper TD10.2, 84 cm away (see Fig. 7). The second group is SC-21-TD10.2. This set comprises two Cretaceous chert elements, a core on flake and a flake, separated 319 cm from each other, whose connecting line is against the general slope of the level. In this case, the exploitation flake is clearly inserted in TD10.2-BB, while the core is located into TD10.2.2, 2 cm below the bottom of the bison bone bed archaeolevel. In both cases, the refitted artefact is in the contact area between different levels; therefore, the limited vertical displacement may be due to minimal post-depositional disturbances of to a punctual misassignment.

The Upper TD10.2 archaeolevel contains all quartzite groups and one sandstone refit. Notable examples of these are two groups featuring two discrete sequences of longitudinal unipolar exploitation, located in the area with the highest density of lithic remains, whose scattering corresponds to what would be expected in a knapping area, as illustrated in Fig. 8b (further details in discussion). In TD10.2.2, only one dorso-ventral connection on quartz has been found, highlighting very different management of raw materials, with fragmented *chaîne opératoires* and the input of artefacts already configured into the cavity (Fig. 8f).

In contrast, TD10.2-BB comprises the entire Cretaceous and Neogene lithic connections and three sandstone refit groups (two of them post-depositional conjoins), emphasising the unique chert specialisation of the archaeolevel and confirming the occurrence of

Table 2
Model performance parameters for each ML algorithm in line M (1 m), by percentage of material trained.

Nº Training Points	Percentage TD10	SVM				RF			
		Sensitivity	Specificity	Accuracy	Kappa	Sensitivity	Specificity	Accuracy	Kappa
329	1%	0.600	0.968	0.908	0.840	0.620	0.970	0.908	0.843
1641	5%	0.664	0.982	0.949	0.911	0.709	0.987	0.961	0.933
3281	10%	0.699	0.985	0.958	0.929	0.834	0.992	0.974	0.956
6561	20%	0.737	0.988	0.964	0.940	0.875	0.994	0.981	0.969
9842	30%	0.763	0.991	0.973	0.954	0.886	0.995	0.983	0.972
13,122	40%	0.811	0.992	0.977	0.961	0.938	0.996	0.990	0.983
16,402	50%	0.805	0.991	0.973	0.954	0.920	0.997	0.990	0.983
19,683	60%	0.846	0.992	0.975	0.959	0.915	0.996	0.985	0.976
22,963	70%	0.856	0.993	0.978	0.963	0.935	0.997	0.990	0.984
26,244	80%	0.877	0.994	0.980	0.967	0.951	0.997	0.991	0.986
29,524	90%	0.890	0.993	0.980	0.967	0.934	0.996	0.992	0.987
32,804	100%	0.904	0.994	0.980	0.967	0.934	0.997	0.992	0.987

Table 3
Lithic connections from sub-unit TD10.2 by raw materials.

	Neogene chert	Cretaceous chert	Quartzite	Sandstone	Quartz
Nº groups	23	39	3	4	1
Pieces refitted	52	137	25	9	2
Nº min. elements	2	2	3	2	2
Nº max. elements	5	20	11	3	2
Mean elements	2.26	3.51	8.34	2.25	2

Table 4
Number of refitting groups and refitted lithic artefacts by archaeolevels. *Artefacts whose refit group is contained in TD10.2-BB but located in adjacent levels.

Raw Material	Upper TD10.2		TD10.2-BB		TD10.2.2	
	Groups	Artefacts	Groups	Artefacts	Groups	Artefacts
Neogene chert	0	0	23	52	0	0
Cret. chert	0	1*	39*	135	0	1*
Quartzite	3	25	0	0	0	0
Sandstone	1	3	3	6	0	0
Quartz	0	0	0	0	1	2
Total	*4*	*29*	*65*	*193*	*1*	*3*

in situ knapping activities. An inside inspection of the refits' vertical distribution has revealed three different patterns of refit alignment. There are 11 refit groups having all their elements at the top of the level (example in Figs. 7), 15 groups whose components are located at the bottom of the level, and another 11 sets with their artefacts in the intermediate part of TD10.2-BB. The remaining groups show their constituent elements scattered along the vertical sequence, or are discarded from the analysis owing to their minimum connection distance.

4.4. TD10.2 occupation sequence

The integration of traditional archaeostratigraphy, supervised ML, and lithic refitting has allowed the sub-unit TD10.2 to be dissected into three main archaeological levels over the entire excavation area. This refined classification includes a total of 87,491 archaeological remains (Table 5 and appendix C).

Upper TD10.2 sublevel (n = 13,717) is spread across the whole excavation surface with a thickness ranging from 45 cm in the northeastern area, to 60 cm in the thickest spots. It presents an average intensity of 159.3 items/m^2, distributed inhomogeneously, with an increasing density towards the east archaeological profile and the northeast corner. This archaeolevel is perfectly delimited from the base of the TD10.1 bone bed in the north area by a mainly sterile line, however, its spacing becomes blurred towards the southwest of the excavated area. The separation between Upper TD10.2 and TD10.2-BB is generally neat and defined by a fall of large blocks. Nevertheless, the boundary between these two levels is sporadically unclear or awkward to trace, especially in areas of higher material density (Figs. 4 and 5). The depositional slope of the materials follows the same topography as the underlying TD10.2-BB level (see below).

A preliminary overview of the technological assemblage reveals a broader representation of quartzite and sandstone materials with respect to TD10.2-BB, although chert remains the predominant raw material (90.77%). No refits have been found in this lithotype, however. Conversely, quartzite is outstanding, with 40.98% (n = 25) of elements refitted.

TD10.2-BB includes 69,310 archaeological items. It presents a very compact line of imbricated remains, with a sparse sedimentary matrix among them. The assemblage has a maximum thickness of 15 cm on the north-eastern section of the site, and decreases towards the south and west to a thickness of about 8 cm. Despite its lesser thickness compared to the preceding Upper TD10.2, the density of archaeological artefacts is substantially higher, with an intensity of 696.28 items/m^2.

This level tilts steeply from west to east, with a gradient of approximately 22% between the west boundary (line 10), and the central area (line 18), thereafter flattening to a slope of about 4%. From north to south, the level also presents a pronounced depositional slope, with an average gradient of 15% in the eastern area. As one moves towards the west, the dip becomes more variable, with slopes reaching 30% in the south and moderating towards the north, smoothing out to 6%. These results are coherent with the description made by Campaña et al. (2016), based on 3D models.

TD10.2-BB discloses a continuous succession of archaeological materials with some undulations and voids due to distortion by medium to large sized limestone blocks. Materials extend from the whole surface, although abundance increases towards the archaeological north and east, matching the slope directions.

Archaeostratigraphic outlining of this level has strengthened the previously observed specialisation in chert, which represents 98.75% (n = 10,604) of the whole lithic assemblage.

Numerous chert refits (n = 188) also reinforce the existence of complete *chaîne opèratoires* in the cavity. The remaining raw materials are circumstantial and are closely related to percussive materials and large formats. Preliminary visual analysis of osteological and lithic remains points to a differential distribution, likely derived from the occurrence of knapping areas not totally coincident with the carcass processing or disposal areas, but an in-depth analytical study is needed to delve deeper into this issue.

Inside level TD10.2-BB, it is noteworthy that in some sections (transversal lines N-M and longitudinal 20–22), two possible sublayers, separated by a very narrow gap line with a lower density of materials, are visible (Fig. 9). Nonetheless, this segmentation cannot be traced along the entire excavation area.

In contrast to the previous levels, TD10.2.2 (n = 4464) displays a very scattered assemblage, with an inhomogeneous distribution throughout the site, mainly concentrated in the SE area of the excavation, where it reaches a thickness of about 50 cm (Fig. 8e and f). Precisely in this area, a significant fall of large blocks has been recorded, along with an archaeostratigraphic alteration, likely caused by bioturbations and a lateral sediment input (Fig. 5c). There is another slight aggregation of materials in the central archaeological area as well as a localised accumulation on the southwestern side. The rest of the materials are distributed in the form of more or less isolated spots along the surface.

5. Discussion

5.1. Methodological considerations

Literature has widely emphasised the importance of dissecting palimpsest to obtain greater spatial and temporal resolution (Dibble et al., 2017; Machado et al., 2015; Malinsky-Buller et al., 2011; Mallol and Hernández, 2016; Mora Torcal et al., 2020; Sañudo et al., 2016; Spagnolo et al., 2016; Way, 2018). Traditionally,

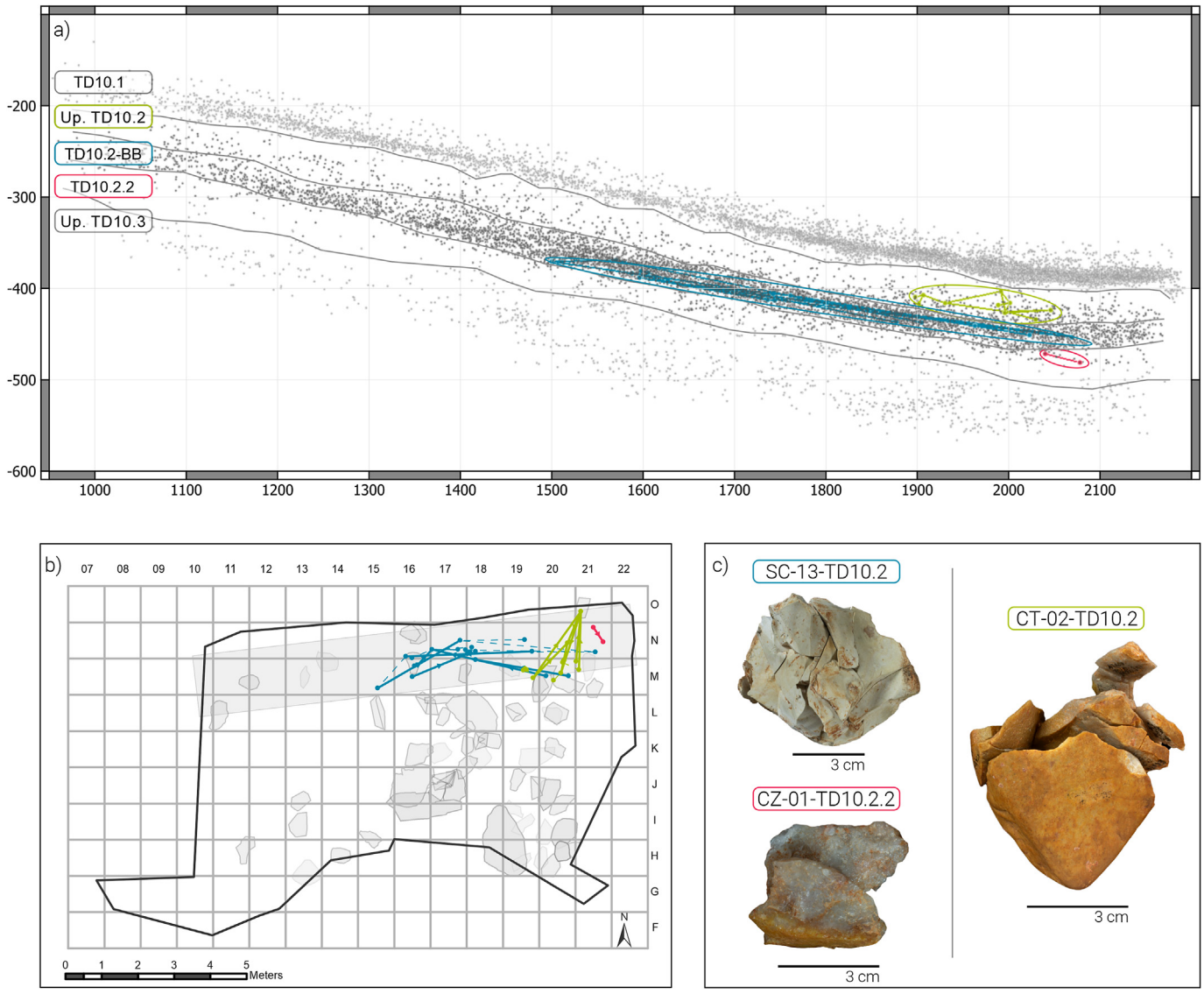

Fig. 6. a) Cross-section with different refit groups. In green, quartzite refit CT-02-TD10.2, from Upper TD10.2 sublevel. In blue, Cretaceous refit SC-13-TD10.2, from TD10.2-BB. In fuchsia, quartz refit CZ-01-TD10.2.2, from TD10.2.2 sublevel. Only lithic artefacts are projected (grey points); b) Horizontal distribution of the selected refit groups. Refits are represented by solid lines that indicate the direction of the link. Conjoins are illustrated with dash lines. The grey polygon represents the section of the vertical profile; c) Refitted groups from TD10.2. Pictures by María Guillén.

the archaeostratigraphical definition of different levels in a site, has been carried out through the visualisation of vertical cross-sections, proving to be a useful technique for isolating different discrete episodes or archaeolevels (Canals et al., 2003; Diez-Martín et al., 2014; Sánchez-Romero et al., 2017; Sañudo et al., 2012). Nevertheless, when confronted with large quantities of remains in homogeneous sediments, and without continuous or evident sterile hiatuses, archaeostratigraphy turns out to be more time-consuming, challenging, and quite subjective. This is particularly noticeable at sites that have a substantial extension, or areas with densely concentrated remains, such as sub-unit TD10.2.

Recent implementation of artificial intelligence has introduced a new quantitative dimension in the archaeological discipline, leading to the potential of automating classification and prediction tasks, while avoiding or minimising noise imposed by the subjective perception of the observer. ML algorithms not only automate and reduce data processing, but also assist in decision-making based on robustly defined mathematical criteria (Bishop, 2006; Goodfellow et al., 2016).

In this research, we have implemented two ML algorithms (*sensu* Martín-Perea et al., 2020), in combination with more traditional techniques for the identification of distinct levels within an archaeological assemblage. The results obtained show the potential of artificially intelligent procedures in the fine-tuning and definition of final archaeostratigraphical models.

Metrics derived from RFs and SVMs (Table 1 and Table A4) demonstrate a positive and robust performance with notably higher confidence in all classification tasks performed. Furthermore, subsequent archaeostratigraphic verification shows vertical and lateral consistency of the different levels. The implementation of lithic refitting provides further assistance for verifying the archaeostratigraphic observations, testing the accuracy and reliability of ML algorithms, proving the vertical integrity of the deposits, and assessing the incidence of post-depositional disturbance processes.

When considering the efficiency of the method outlined in this

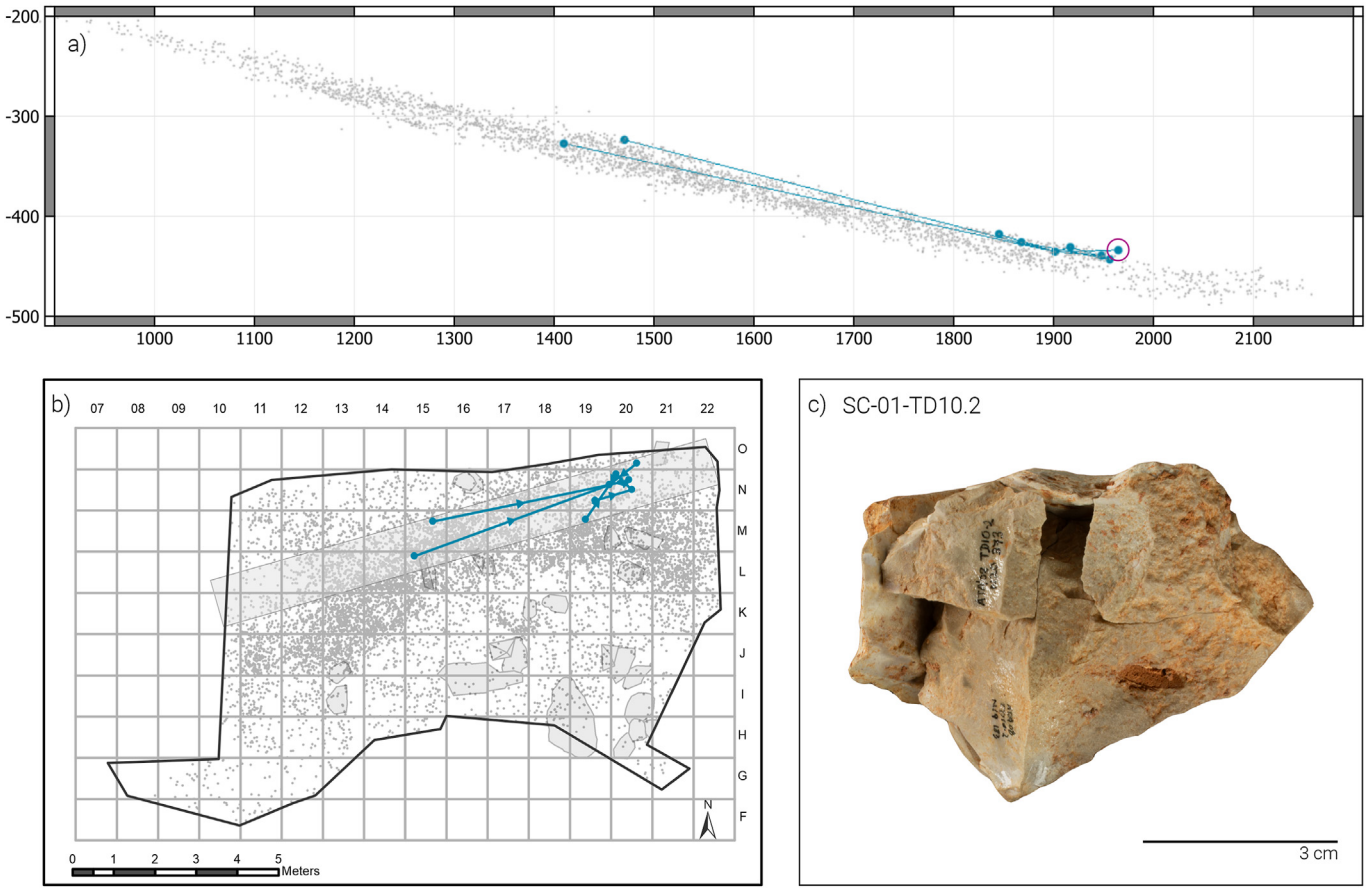

Fig. 7. a) Vertical distribution of SC-01-TD10.2 Cretaceous refit, projected over TD10.2-BB lithic and faunal remains (grey points). Note how all the elements scatter on the top of the subunit, with the exception of one flake (encircled), ascribed to Upper TD10.2; b) Horizontal distribution of SC-01-TD10.2. Grey dots indicate the distribution of lithic artefacts from sub-unit TD10.2-BB. The grey polygon represents the section of the vertical profile; c) Picture of SC-01-TD10.2, by María Guillén.

paper, in comparison with other palaeontological sites where similar approaches were adopted (Batallones 3: Martín-Perea et al., 2020, 2021a; Batallones 10: Martín-Perea et al., 2020, 2021b; and Venta Micena 4: Luzón et al., 2021), slightly different results have been obtained. Firstly, it should be noted that a previous archaeostratigraphic dissection using more traditional approaches was opted for this study, as opposed to the unsupervised expert-in-the-loop system proposed by Martín-Perea et al. (2020, pp. 4–5). This decision was motivated firstly by the advanced state of visual archaeostratigraphical analysis, and secondly, by the unsuccessful results of unsupervised learning in this particular case study.

By conducting a first review by means of cross-section observation, a certain degree of qualitative bias has been introduced into the classification. Nevertheless, in the referred work, although a first automated phase of cluster detection is involved, a subsequent decision-making process by the researcher is still required (Martín-Perea et al., 2020, p. 6). Moreover, as detailed in Table 2, a very large number of pre-assigned materials is not necessary to obtain high performance results in the ensuing computational processing. Therefore, only those points with a trustworthy assignment can be chosen for training, leaving all other data that present uncertainties as indeterminable, so as to control and minimise potential bias in the process.

In Batallones 3 (Martín-Perea et al., 2021a), Batallones 10 (Martín-Perea et al., 2021b) and Venta Micena 4 (VM4), (Luzón et al., 2021), high agreement rates between algorithms were highlighted, with RF being the most decisive and confident classifier. Conversely, although the mean values of the trained models from the present study are minimally better in RF, SVM is the algorithm with the highest decision power for classification.

In all these paleontological sites, κ values for the overall assessment of system inter-rate reliability vary between 0.75 for Batallones 3 to 0.85 for VM4. Our model, however, yields a value below the expected threshold for a nearly perfect agreement. Nevertheless, although the present calculated κ is lower, the percentage of classified material is significantly higher compared to Batallones 3.

These slightly weaker values may be attributed to the intrinsic nature of the present case study. Firstly, the number of points analysed for the archaeostratigraphic study of TD10 sequence is noticeably higher than those of the sites compared. VM4 and Batallones 10, which have the best performance, contain less than 8,000 fossil elements. Batallones 3, with more than 16,000 remains, yields a higher number of indeterminate points and a lower accuracy rate for the model. Secondly, surface area of TD10 is significantly larger than these deposits, which can lead to a greater lateral and vertical variability. Thirdly, all three palaeontological sites undergo different post-depositional processes from those derived from the karst cave system of Gran Dolina. These studies report rapid sedimentation rates and excellent preservation of remains for Batallones, with most of the individuals in anatomical connection (Martín-Perea et al., 2021b), or low to moderate disturbance impact for the open-air site of VM4 (Luzón et al., 2021).

Finally, TD10 is an archaeological deposit, as opposed to palaeontological, which likely increases the complexity of the accumulation, abandonment, and reuse dynamics of the site due to

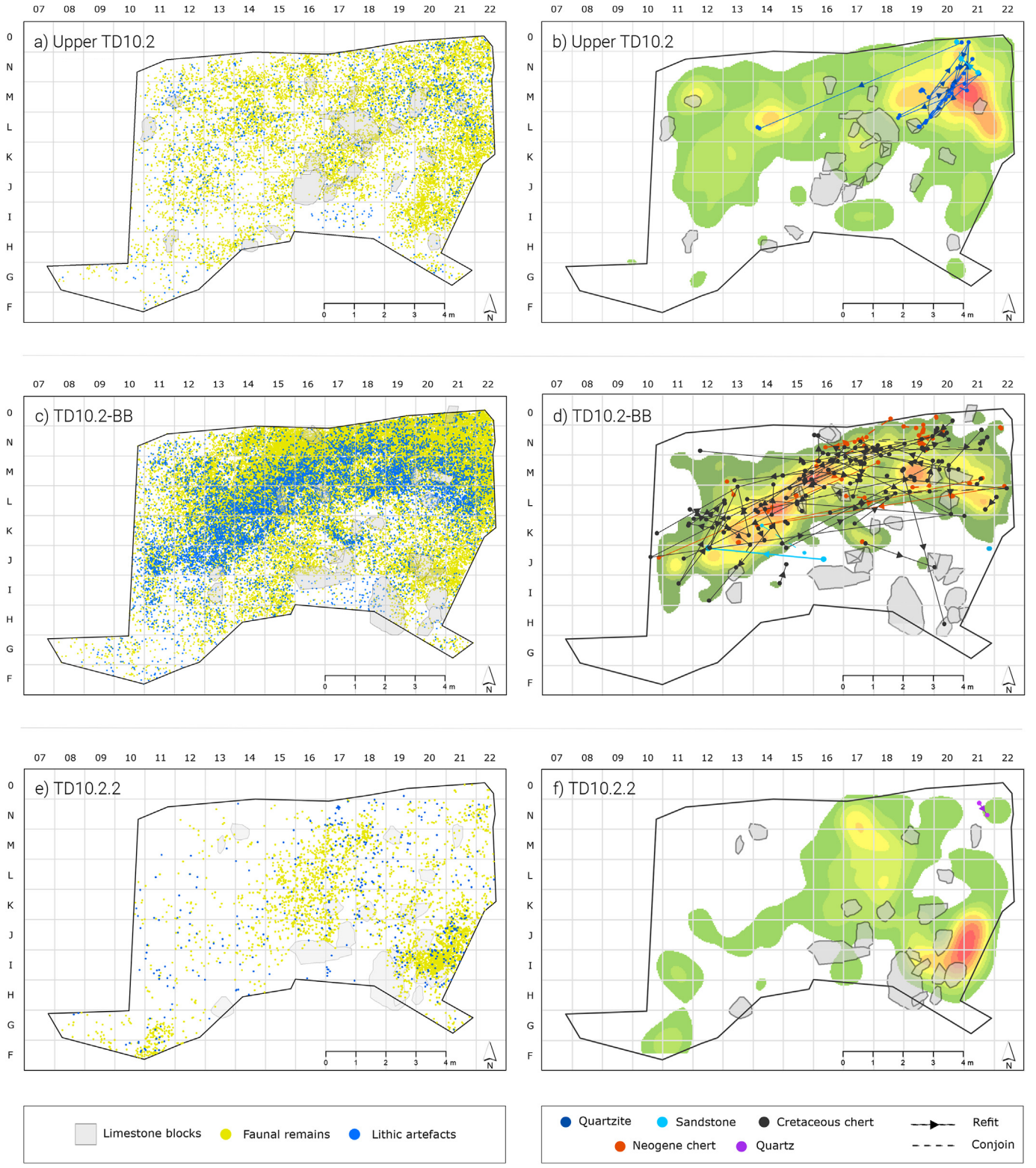

Fig. 8. Left column: Horizontal distribution patterns of the TD10.2 levels: a) Upper TD10.2, c) TD10.2-BB, e) TD10.2.2. Yellow colour for faunal remains and blue for lithic artefacts. Limestone blocks larger than 50 cm are drawn. Right Column: Spatial distribution of lithic connections by raw materials: b) Upper TD10.2, d) TD10.2-BB, f) TD10.2.2. Refits are indicated with a solid line and conjoins with a dotted line. Arrows indicate the artefact's movement direction within a refit group. The base map shows the Kernel density estimation of lithic remains (performance with Arcmap software).

Table 5
Osteological and lithic artefacts classified by archaeolevels within sub-unit TD10.2.

	Upper TD10.2	TD10.2-BB	TD10.2.2	Total
Fauna remains	12,179	58,572	3993	74,744
Lithic artefacts	1538	10,738	471	12,747
Total	*13,717 (15.68%)*	*69,310 (79.22%)*	*4464 (5.10%)*	*87,491*

hominin activity. Archaeological artefacts are deposited through adaptive systems, subject of both cultural and natural processes, thus affecting the separation between different events (Schiffer, 1983, 1975). While unsupervised pattern recognition tasks have proven highly useful in palaeontological contexts, in the specific case of TD10.2 sequence, a shorter time-scale, and thus higher

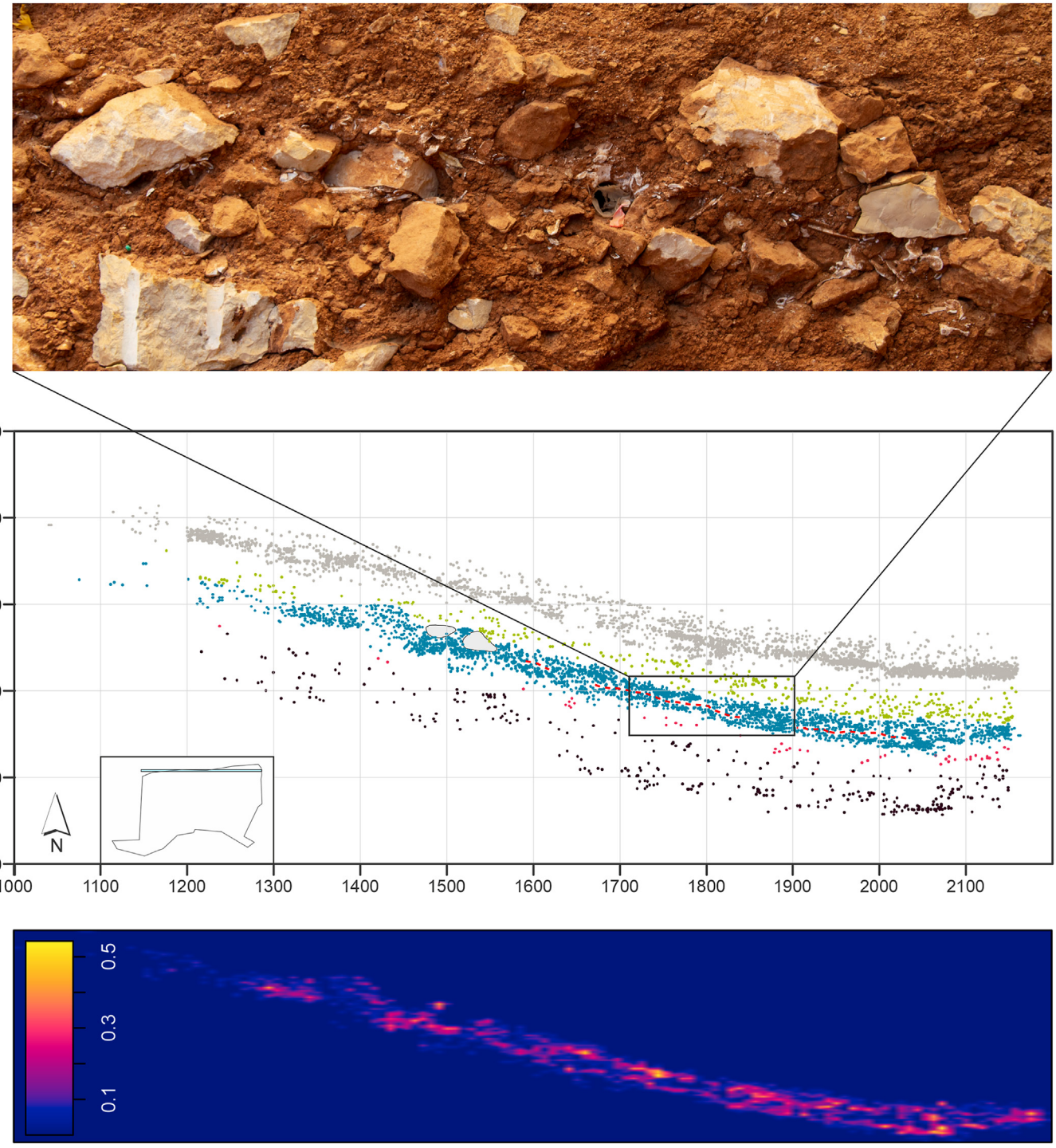

Fig. 9. Detail of TD10.2-BB in the North archaeological profile and 20 cm thick cross section (Line N, Y coord. 1360–1380). Note how at some spots two distinct layers are visible (red dotted lines). Picture by María D. Guillén. At the bottom, Kernel density map with osteological and lithic remains of TD10.2-BB (same cross-section), performed with "bw.diggle" function (sigma = 1.140), in the Spatstat package (Baddeley et al., 2015).

resolution is required to dissect human activities and making behavioural inferences (Brooks et al., 1982; Diez-Martín et al., 2014; Vaquero et al., 2012).

The application of supervised ML algorithms could be strengthened by the integration of new variables in the training data, such as taxonomic representation, raw material information, and taphonomic analysis, among others. Nevertheless, to contemplate the introduction of new data inputs, an initial knowledge of the peculiarities of each archaeological level would be required. Therefore, this second step can be considered for refining previous archaeostratigraphic work in the pursuit for higher resolution, but not for a preliminary dissection of archaeological units.

5.2. The spatio-temporal resolution of TD10.2

The different archaeolevels included in TD10.2 display a diverse nature, leading us to consider their integrity and degree of spatial and temporal resolution to raise the pertinent questions and objectives to be addressed when studying each one of them.

5.2.1. Upper TD10.2

Upper TD10.2 stands out as a distinct entity, clearly different from the bone beds that vertically enclose it. As a rule, it is feasible to map and delimit it along the whole archaeological surface due to the density change in relation to the adjacent levels. The application of various archaeostratigraphic techniques, however, has not been conclusive in untangling the deposit, making it unfeasible to distinguish sequences of events. From this perspective, the archaeological level of Upper TD10.2 presents an unclear scenario, with an aggregation of diverse materials, possibly derived from the lumping and mixing of several archaeological and post-depositional accumulative and/or erosive events that occurred over an undetermined time span.

These observations are consistent with the definition of an accumulative palimpsest (*sensu* Bailey, 2007). This type of palimpsest is commonly observed in Palaeolithic contexts and represents the aggregation and overlapping of different discrete activities and events into a single package, involving time-averaged occupations that cannot be disentangled into individual episodes. As pointed out by Bailey (2007, p. 204), "it is entirely possible that occasional high spots of patterning representing individual episodes may be preserved at random, unaffected by the mixing process" . The same phenomenon can be observed in Upper TD10.2, where, among all the materials, we can still detect discrete knapping episodes evidenced by lithic refits.

Noteworthy examples are two groups of quartzite refits, comprising 11 items respectively, featuring longitudinal unipolar exploitation sequences. CT-02-TD10.2 contains almost the entire reduction sequence, from the introduction of a small nodule into the cavity until its subsequent abandonment (see Fig. 6). CT-01-TD10.2 represents an intermediate step of the exploitation process, but the core and final products are absent. The location of these refit groups, in the peripheral area and close to the artificial walls of the excavation, does not allow us to confidently formulate behavioural inferences, as we are unable to discern if the lack of certain artefacts is due to an intentional anthropic action (e.g., transported tool-kit) or they are buried in an unexcavated area of the cavity.

Both quartzite set's spatial distribution and average distances suggest anthropogenic spots remaining relatively intact within the archaeostratigraphic unit (Fig. 8b). Despite a certain displacement of the artefacts, the radios and scattering of those groups correspond to what would be expected in a knapping area, with an average distance of 165 cm for CT-01-TD10.2, and 82 cm for CT-02-TD10.2 (Bargalló et al., 2018; de la Torre et al., 2019; Kvamme, 1997; Newcomer and Sieveking, 1980; Zorrilla-Revilla et al., 2021).

The last quartzite set (CT-03-TD10.2) involves a small retouch flake located into the densest concentration of lithic remains, close to the aforementioned refits and a tool on a large flake, split in two by a transversal fracture after its shaping. The latter are located more than 7 m away, in a second area of clustered lithic remains (Fig. 8a–b). The shaping sequence, distance, and distribution of the artefacts, suggest a possible intentional movement from a knapping area to a use area (or eventual final abandonment) (Bargalló et al., 2020; López-Ortega et al., 2017; Vaquero et al., 2017).

Regardless of the identification of discrete episodes and isolated individual occurrences, however, these insights remain anecdotal within the general Upper TD10.2 picture. Understanding formation processes, time recorded, or site's functionality, requires micromorphological and sedimentological analyses, accompanied by in-depth zooarchaeological, taphonomic, and technological studies to be carried out in the forthcoming research.

5.2.2. The Bison bone bed

TD10.2-BB exhibits very different conditions from those discussed for the overlying level. The archaeostratigraphic observation, the preliminary analysis of the refits and the technological assemblage, and the previous zooarchaeological and taphonomic studies, enable us to characterise this deposit as a palimpsest but with a high degree of temporal and spatial resolution (*sensu* Mora Torcal et al., 2020; Sañudo et al., 2016), likely reflecting features in line with the "rapid-accumulation" model proposed by Malinsky-Buller et al. (2011, p. 90).

Taphonomic analysis of TD10.2-BB faunal remains reveals minimal post-depositional bone surface alterations, reflecting optimal preservation conditions of the deposit (Rodríguez-Hidalgo, 2015; Rodríguez-Hidalgo et al., 2017, p. 95). Apart from the occurrence of manganese oxide precipitation, which is widespread across the whole assemblage, and subaerial modifications (sensu Capaldo, 1997), which are rare and never exceed 2% of the analysed material, the scarcity of hydric runoff exposure traces, like surface abrasion or rounding, suggests a stable sedimentary environment, unaffected by high-energy post-depositional processes. Nevertheless, an area with a small channel of low-energy water circulation has been documented (Rodríguez-Hidalgo et al., 2017), but its degree of impact is low.

Macroscopic observation of bone and lithic surfaces (excluding Neogene chert altered by chemical desilicification) reveals fresh ridges and edges with no discernible traces of rounding, polishing, or abrasion, despite of being (in the case of chert) entirely covered by a well-developed whitish patina. Additionally, edge examination supported by use-wear analysis indicates no significant trampling damage. This observation coincides with the faunal taphonomic results, which return minimal evidence of trampling (Rodríguez-Hidalgo, 2015), and with the vertical integrity found in most lithic refits.

All these modifications display a preferential distribution in the northern sector of the excavation (Rodríguez-Hidalgo, 2015, p. 134), corresponding with the highest density of faunal remains. Future studies would be needed to clarify whether this higher concentration of remains is attributable to the presumed anthropogenic configuration of the space, or to other phenomena such as the cumulative effect of post-depositional processes. Solely the presence of root etching, again anecdotal, exhibits a different distribution, with one concentration at the entrance of the cavity and another in the northeast corner of the archaeological surface (Rodríguez-Hidalgo, 2015, p. 135). The latter presumably implies the existence of a roof opening, providing natural light into the deepest area of the site. Interestingly, the two refit pieces placed in adjacent sublevels (see section 4.4) are located in these root-

affected areas, which may explain their slight vertical displacement (Deschamps and Zilhão, 2018; Wood and Johnson, 1978).

Regarding the integrity of the level (Binford, 1981b, p. 19), preliminary technological analyses reveal the existence of nearly complete *chaîne opèratoires,* with a high percentage of microdebris and small flake products, and evidence of resharpening activities that reinforce the idea of intensive knapping processes developed *in situ* (Arteaga-Brieba et al., 2020; Ollé et al., 2013). Spatial analysis of the lithic connection distribution unveils the preservation of discrete knapping episodes (see Fig. 8d), supporting the idea that, despite minor postdepositional affections, the remains are close to their primary position (Arteaga-Brieba et al., 2021). Furthermore, their vertical distribution shows, in most cases, a high intra-level consistency and stratigraphic integrity, being able even to isolate discrete phases within level TD10.2-BB.

Additionally, there is a high prevalence of axial elements, low-survival items, such as ribs, and elements with reduced visibility in other Pleistocene sites, such as hyoid bones (Rodríguez-Hidalgo, 2015; Rodríguez-Hidalgo et al., 2017), further supporting the evidence of the high integrity of this assemblage. However, as pointed out before, a moderate incidence of carnivore scavenging is documented.

One of the initial questions when addressing this research was to attempt to estimate the number of hunting and carcass processing events that took place in TD10.2-BB. Unfortunately, the archaeostratigraphic data obtained do not support this distinction, as it does not offer the desired degree of technical resolution. The intensity of the occupation and the sediment compaction prevents the division of the assemblage at present, while it may be necessary to develop new, more precise methods, for obtaining a greater precision in distinguishing between different episodes and activities within assemblages of these characteristics.

Nevertheless, evidence of possible sublayers in archaeolevel TD10.2-BB have been detected, allowing us to reject the hypothesis of a single occupation event and to consider the temporal framework of the deposit. Data provided by dental eruption, meso- and micro-wear patterns, reveal that bison were slaughtered in two separate seasonal windows, each followed by periods of low or non-anthropogenic activity (Rodríguez-Hidalgo et al., 2016). These results lead to two possible scenarios: a) a succession of short and recurrent occupations during early spring and autumn seasons, or b) a few occupations of longer duration but seasonally limited (Rodríguez-Hidalgo et al., 2016, p. 788).

The archaeostratigraphic visualisation of the seasonality data (Fig. 10) does not yield any strong evidence to support the identification of occupational events. Seasonality estimators, albeit numerous ($n = 45$), represent a tiny percentage of the whole assemblage and do not facilitate statistical inferences. Nevertheless, certain trends can be observed, with a predominance of spring signals at the bottom of the bison bed horizon, and autumn indicators at the top. The density plot (Fig. 10d) also suggests the same pattern. Although there is an overlapping, the two seasonal peaks show a separation, with a dominance of spring markers at higher depths than the autumn ones.

This outcome leads to two possible interpretations; a) there is temporal isolation (at least partial) between one or more events occurring in spring, followed by autumn events, or b) there is a certain spatial separation between the episode(s) that occurred in spring (preferably located at lower depths of the cavity) and the episode(s) that occurred in autumn. This second explanation seems less plausible since, firstly, the plan view of the remains (Fig. 10c) does not sustain this hypothesis and, secondly, most of the seasonal data are located in the flatter excavated area. Therefore, the slope does not appear to play a relevant role in the vertical spacing observed.

The vertical distribution of the refits in different elevations also sheds light on the minimum number of occupational events (calculated at two), which are consistent with archaeostratigraphic observations (Fig. 9), and seasonality information. To date, the available data do not allow us to further estimate the number of occupations in TD10.2-BB. Nevertheless, several strands of evidence support the second scenario drawn by the seasonality patterns: few but intense occupations of longer duration and seasonally limited. Catastrophic mortality patterns, associated with mass predation events, rule out the occurrence of isolated prey-hunting episodes (Rodríguez-Hidalgo et al., 2017). The limited variability of the assemblage in both taxonomic and raw material composition may also reflect low episodes of occupation, considering that both the temporal factor and the recurrence of occupations are sources that introduce variability in the archaeological record (Shott, 2008; Vaquero et al., 2012). Finally, the high density of anthropogenically modified remains and evidence of recurrent *in situ* knapping activities suggest prolonged or very high intensity occupations (Barton and Riel-Salvatore, 2014; Kuhn and Clark, 2015).

In sum, the cumulative evidence suggests that TD10.2-BB, despite being a palimpsest in the strict sense, possesses enough resolution and integrity to warrant behavioural insights to be made. The recurrence of the same function over time and the low incidence of post-depositional disturbances have allowed the assemblage to largely reflect the tasks carried out in the cavity. While the occurrence of other activities cannot be ruled out, these have little or no visibility in the current archaeological record. Indeed, the features of TD10.2-BB allow for an analysis on a nearly individual scale (based on lithic refits), as well as on a larger temporal scale, by approaching the preneandertal bison-hunters' subsistence strategies, cultural dynamics, or social complexities.

5.2.3. TD10.2.2

The casuistic of archaeolevel TD10.2.2 is completely different from that of TD10.2-BB. This assemblage has been defined as an intermediate level between the TD10.3 lithostratigraphic sub-unit and the bison-bone bed horizon. The archaeological materials are patchy along the cavity surface, while it is hard to determine if there is any synchronic association between them. Furthermore, the southeast area, with the highest density of materials, is associated with a block fall and a lateral sedimentary input, causing significant disturbances and remobilisation of materials.

The low density of archaeological remains in comparison with the other levels, as well as their scattered distribution, may be indicative of short and sporadic cavity occupations, with dynamics probably similar to those interpreted for Upper TD10.1 (Saladié et al., 2018). A unique quartz refit reveals a punctual knapping gesture, but it is an isolated occurrence, which evidences the high degree of fragmentation of the *chaîne opèratoires*. As has been pointed out for Upper TD10.2, an in-depth study of the faunal and lithic composition is required to further understand the nature of this level.

Nevertheless, the separation of this assemblage within the TD10.2 sub-unit and the analysis of its vertical dispersion, enabled us to define the deposit as a true palimpsest, with significant post-depositional modifications, which makes it unsuitable for drawing behavioural inferences on a small temporal scale. Nevertheless, its distinction within TD10.2 represents a breakthrough in the understanding of technological evolution and occupation patterns across the TD10 sequence.

6. Conclusions

Recognising the temporal and spatial scale of archaeological assemblages is a critical issue for formulating behavioural

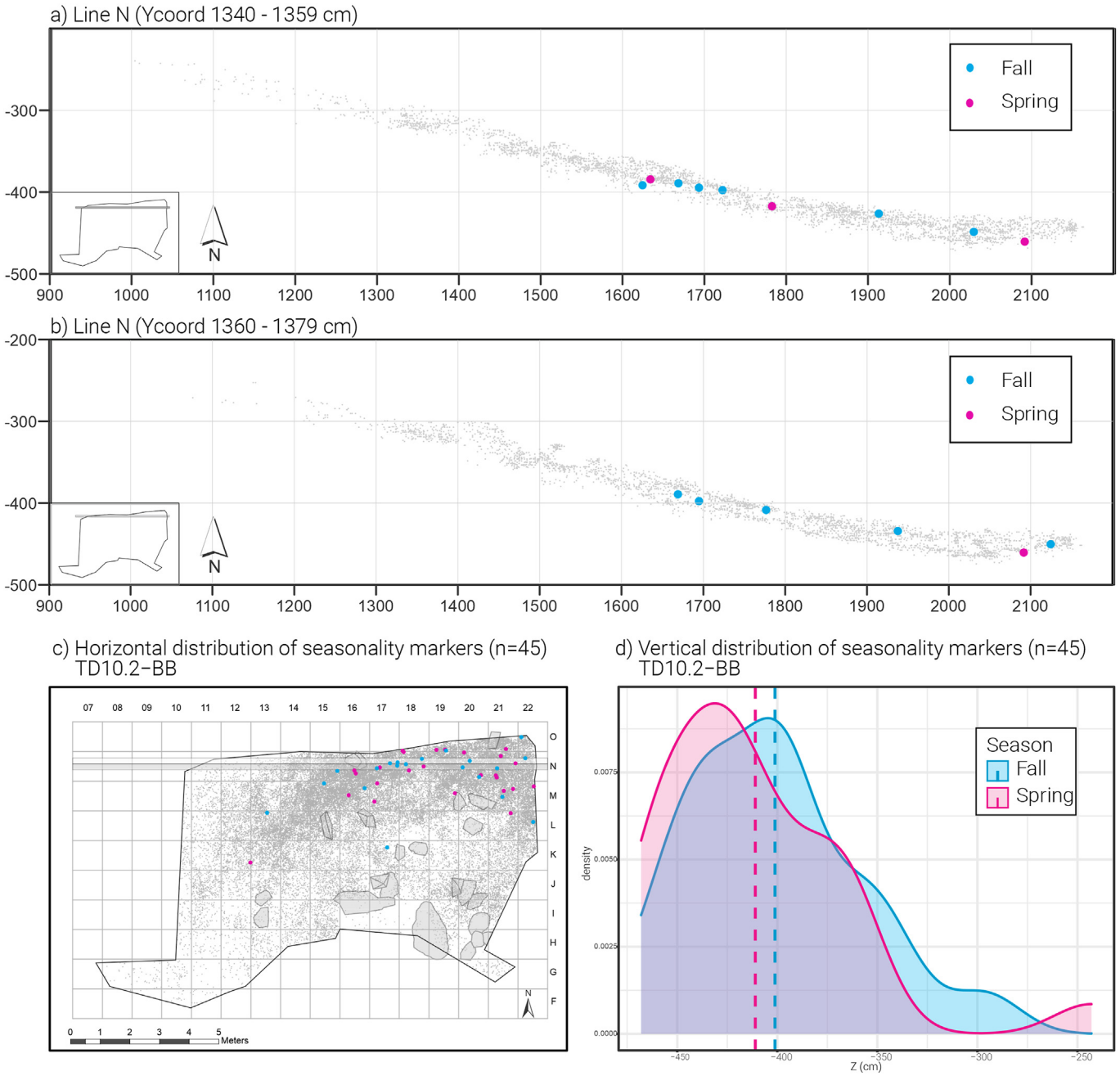

Fig. 10. At the top, cross-sections of TD10.2-BB level with seasonality data. The profiles with the most data available have been selected; c) Horizontal spread of seasonality markers, plotted over the distribution of TD10.2-BB fauna remains (in grey); d) Vertical distribution of seasonality markers from TD10.2-BB.

inferences and deeper, more comprehensive, interpretations of the past. Particularly when dealing with palimpsests, an exhaustive data recording system is stressed, with accurate techniques that allow their eventual virtual reconstruction and enable palaeoethnographic readings.

Classical archaeostratigraphic methods remain a fundamental first step in discerning between several events or significant formation episodes; however, these studies are time-consuming (especially for extensive surface excavations), and can be challenging if there are no noticeable gaps among levels. Therefore, additional possibilities have been explored to complement this initial approach.

This study has shown how applying ML algorithms is a powerful technique for automating these types of analyses, while reducing sample processing time, and providing a robust quantitative tool for associating fossils and artefacts from problematic areas to their corresponding levels. Needless to say, it is imperative to start with reliable and verified data, as this will have a notable impact on the quality of results and algorithm performance.

From an archaeostratigraphic standpoint, the contribution of the refits becomes essential for recognising formation processes and post-depositional modifications, understanding the internal chronology of each assemblage, and confirming previous observations of the archaeostratigraphic record, as well as the spatio-temporal integrity of the deposit.

The combination of these three proxies has proved to be very

effective for the analysis of the TD10.2 sub-unit, allowing us to define three main assemblages with diverse resolutions and compositions. Upper TD10.2 and TD10.2.2 are palimpsests with a low degree of temporal resolution, although the first level still contains vestiges of isolated activities. TD10.2-BB, on the other hand, has been defined as a high spatiotemporal resolution palimpsest. The analysis of its vertical dimension has led to the identification of (at least) two main formation and occupational events, both of which are integrally related to seasonal anthropogenic subsistence practices.

Mass communal hunting techniques have no analogues or are barely discernible in Lower Palaeolithic sites. We have a remarkable opportunity to acquire a deeper knowledge of these exceptional communal hunting activities owing to the high resolution of TD10.2-BB. The potential to draw cultural and behavioural inferences is improved by the high visibility of the activities undertaken and their reflection in the spatial organisation. A more thorough examination of the particular idiosyncrasies of this assemblage will be possible through future technological, traceological, and spatial studies.

Credit author statement

Andion Arteaga-Brieba: Conceptualisation, methodology, Data curation, Formal analysis, Visualisation, Writing-Original draft preparation. Lloyd A. Couternay: Methodology, Software, Writing-Reviewing and Editing. Lucía Cobo-Sánchez: Conceptualisation, Writing- Reviewing and Editing. Antonio Rodriguez-Hidalgo: Writing- Reviewing and Editing. Palmira Saladié; Writing-Reviewing and Editing. Andreu Ollé; Supervision, Writing-Reviewing and Editing. Marina Mosquera: Project administration, Supervision, Writing- Reviewing and Editing.

Declaration of competing interest

The authors declare that they have no known competing financial interests or personal relationships that could have appeared to influence the work reported in this paper.

Data availability

Data will be made available on request.

Acknowledgements

The archaeological fieldwork at Atapuerca is supported by Junta de Castilla y León and Fundación Atapuerca. This research has been developed within the frame of the projects PID 2021-122355NB-C32 (MICINN-FEDER), SGR 2021-01239 (AGAUR) and 2022PFR-URV-64 (URV). A. Arteaga-Brieba is the beneficiary of a predoctoral fellowship from Gobierno de Navarra/Nafarroako Gobernua. L.A. Courtenay is funded by the Spanish Ministry of Science, Innovation and Universities, with an FPI Predoctoral Grant (Ref. PRE 2019-089411), associated with the project RTI 2018-099850-B-I00 and the University of Salamanca. A. Rodríguez-Hidalgo is supported by the Spanish Ministry of Science and Innovation through the “María de Maeztu” (CEX2019-000945-M).Institut Català de Paleoecologia Humana i Evolució Social (IPHES-CERCA) has received financial support from the Spanish Ministry of Science and Innovation through the “María de Maeztu” program for Units of Excellence (CEX 2019-000945-M). We also want to thank the Atapuerca research team and María D. Guillén for her assistance with the photographic documentation of the lithic material.

Appendix A. Supplementary data

Supplementary data to this article can be found online at https://doi.org/10.1016/j.quascirev.2023.108033.

References

Adler, D.S., Prindiville, T., J., Conard, N.J., 2013. Patterns of spatial organization and land use during the eemian intergalcial in the rhineland: new data from wallertheim, Germany. Euras. Prehist. 1, 25–78.
Anderson, K.L., Burke, A., 2008. Refining the definition of cultural levels at Karabi Tamchin: a quantitative approach to vertical intra-site spatial analysis. J. Archaeol. Sci. 35, 2274–2285. https://doi.org/10.1016/j.jas.2008.02.011.
Archer, W., Djakovic, I., Brenet, M., Bourguignon, L., Presnyakova, D., Schlager, S., Soressi, M., McPherron, S.P., 2021. Quantifying differences in hominin flaking technologies with 3D shape analysis. J. Hum. Evol. 150, 102912. https://doi.org/10.1016/j.jhevol.2020.102912.
Arnold, L.J., Demuro, M., Parés, J.M., Pérez-González, A., Arsuaga, J.L., Bermúdez de Castro, J.M., Carbonell, E., 2015. Evaluating the suitability of extended-range luminescence dating techniques over early and Middle Pleistocene timescales: published datasets and case studies from Atapuerca, Spain. Quat. Int. 389, 167–190. https://doi.org/10.1016/j.quaint.2014.08.010.
Arriaza, M.C., Domínguez-Rodrigo, M., 2016. When felids and hominins ruled at Olduvai Gorge: a machine learning analysis of the skeletal profiles of the non-anthropogenic Bed I sites. Quat. Sci. Rev. 139, 43–52. https://doi.org/10.1016/j.quascirev.2016.03.005.
Arteaga-Brieba, A., Asryan, L., Mosquera, M., Ollé, A., 2020. The lithic assemblage of the Gran Dolina-TD10.2 kill-butchering site (Sierra de Atapuerca, Spain). In: Book of Abstracts of the ESHE Meeting 2020, p. 6.
Arteaga-Brieba, A., Mosquera, M., Ollé, A., 2021. Connecting things: refits at gran Dolina TD10.2. In: Gómez de Soler, B., Soto, M., Chacón, M.G., Soares, M. (Eds.), Rock and Roll: 13th International Symposium on Knappable Materials, p. 106. Tarragona.
Ashton, N., 2004. The role of refitting in the British Lower Palaeolithic: a time for reflection. In: Walker, E.A., Wenban-Smith, F., Healey, F. (Eds.), Lithics in Action. Oxford, pp. 57–64.
Asryan, L., Ollé, A., Arteaga-Brieba, A., Martín-Viveros, J.I., Fernández-Marchena, J.L., Mosquera, M., 2022. Microwear study of Gran Dolina TD10.2 subunit lithic assemblage (Sierra de Atapuerca, Spain). In: Tracing Social Dynamics. Book of Abstracts. Barcelona, p. 40.
Asryan, L., Ollé, A., Arteaga-Brieba, A., Martín-Viveros, J.I., Fernández-Marchena, J.L., Mosquera, M., 2021. What does the functional study of the lithic artefacts of a kill-butchery site tell us? A case study from the Gran Dolina TD10.2 subunit (Atapuerca, Spain). In: Bouzouggar, A., Boudad, L., Masfour, A., El Faleh El, M., Atki, M., Benbaqqal, H., Segaoui, F. (Eds.), Evolution Des Sociétés Humaines de La Préhistoire à La Protohistoire. UISPP2021 Book of Abstracts, pp. 76–77. Meknès.
Baddeley, A., Rubak, E., Turner, R., 2015. Spatial Point Patterns. Methodology and Applications with R. Chapman and Hall/CRC, New York.
Bailey, G., 2007. Time perspectives, palimpsests and the archaeology of time. J. Anthropol. Archaeol. 26, 198–223. https://doi.org/10.1016/j.jaa.2006.08.002.
Bailey, G., 1983. Concepts of time in quaternary prehistory. Annu. Rev. Anthropol. 12, 165–192.
Bailey, G., 1981. Concepts, time-scales and explanations in economic prehistory. In: Sheridan, G., Bailey, G. (Eds.), Economic Archaeology: towards an Integration of Ecological and Social Approaches, vol. 96. British Archaeological Report International Series, Oxford, pp. 97–117.
Bailey, G., Galanidou, N., 2009. Caves palimpsests and dwelling spaces: examples from the upper palaeolithic of south-east europe. World Archaeol. 41, 215–241. https://doi.org/10.1080/00438240902843733.
Bamforth, D.B., Becker, M., Hudson, J., 2005. Intrasite spatial analysis, ethnoarchaeology, and paleoindian land-use on the great plains: the allen site. Am. Antiq. 70, 561–580.
Bargalló, A., Gabucio, M.J., Gómez de Soler, B., Chacón, M.G., Vaquero, M., 2020. Rebuilding the daily scenario of Neanderthal settlement. J. Archaeol. Sci. Rep. 29, 102139. https://doi.org/10.1016/j.jasrep.2019.102139.
Bargalló, A., Gabucio, M.J., Rivals, F., 2016. Puzzling out a palimpsest: testing an interdisciplinary study in level O of Abric Romaní. Quat. Int. 417, 51–65. https://doi.org/10.1016/j.quaint.2015.09.066.
Bargalló, A., Mosquera, M., Lorenzo, C., 2018. Identifying handedness at knapping; an analysis of the scatter pattern of lithic remains. Archaeol. Anthropol. Sci. 10, 587–598. https://doi.org/10.1007/s12520-016-0378-0.
Barton, C.M., Riel-Salvatore, J., 2014. The formation of lithic assemblages. J. Archaeol. Sci. 46, 334–352. https://doi.org/10.1016/j.jas.2014.03.031.
Berger, G.W., Pérez-González, A., Carbonell, E., Arsuaga, J.L., Bermúdez de Castro, J.M., Ku, T.L., 2008. Luminescence chronology of cave sediments at the Atapuerca paleoanthropological site, Spain. J. Hum. Evol. 55, 300–311. https://doi.org/10.1016/j.jhevol.2008.02.012.
Bickler, S.H., 2021. Machine learning arrives in archaeology. Adv. Archaeol. Pract. 9, 186–191. https://doi.org/10.1017/aap.2021.6.
Binford, L.R., 1981a. Behavioral archaeology and the “pompeii premise. J. Anthropol. Res. 37, 195–208.
Binford, L.R., 1981b. Bones: Ancient Men and Modern Myths. Academic Press, New

York. https://doi.org/10.1016/C2013-0-07180-0.
Bishop, C.M., 2006. Pattern Recognition and Machine Learning. Springer, Singapore. https://doi.org/10.1007/978-3-030-57077-4_11.
Blain, H., Bailon, S., Cuenca-Bescós, G., Arsuaga, J.L., Bermúdez de Castro, J.M., Carbonell, E., 2009. Long-term climate record inferred from early-middle Pleistocene amphibian and squamate reptile assemblages at the Gran Dolina Cave, Atapuerca, Spain. J. Hum. Evol. 56, 55–65. https://doi.org/10.1016/j.jhevol.2008.08.020.
Blasco, R., Rosell, J., Fernández Peris, J., Arsuaga, J.L., Bermúdez de Castro, J.M., Carbonell, E., 2013. Environmental availability, behavioural diversity and diet: a zooarchaeological approach from the TD10-1 sublevel of gran Dolina (Sierra de Atapuerca, Burgos, Spain) and bolomor cave (Valencia, Spain). Quat. Sci. Rev. 70, 124–144. https://doi.org/10.1016/j.quascirev.2013.03.008.
Bordes, J., 2003. Lithic taphonomy of the Châtelperronian/Aurignacian interstratifications in Roc de Combe and Le Piage. In: Zilhão, J., D'Errico, F. (Eds.), The Chronology of the Aurignacian and of the Transitional Technocomplexes: Dating, Stratigraphies, Cultural Implications, pp. 223–244. Lisbon.
Breiman, L., 2001. Random forests. Mach. Learn. 45, 5–32. https://doi.org/10.1007/978-3-030-62008-0_35.
Brooks, R.L., Bettinger, R.L., Borrero, L.A., Bronitsky, G., Brown, K.L., Carlson, D.L., Clegg, J., Ihm, P., Marchese, R.T., Pokotvlo, D.L., 1982. Events in the archaeological context and archaeological explanation [with comments and replies]. Curr. Anthropol. 23, 67–75.
Bustos-Pérez, G., Baena, J., 2021. Predicting flake mass: a view from machine learning. Lithic Technol. 46, 130–142. https://doi.org/10.1080/01977261.2021.1881267.
Butzer, K.W., 1982. Archaeology as Human Ecology. Methods and Theory for a Contextual Approach, Archaeology as Human Ecology. Cambridge University Press. https://doi.org/10.1017/cbo9780511558245.
Campaña, I., 2018. Estratigrafía y sedimentología del yacimiento de Gran Dolina (Sierra de Atapuerca, Burgos). Universidad de Burgos.
Campaña, I., Benito-Calvo, A., Pérez-González, A., Ortega, A.I., Bermudez de Castro, J.M., Carbonell, E., 2016. Using 3D models to analyse stratigraphic and sedimentological contexts in archaeo-palaeo-anthropological pleistocene sites (Gran Dolina site, Sierra de Atapuerca). In: CAA2015. Keep the Revolution Going: Proceedings of the 43rd Annual Conference on Computer Applications and Quantitative Methods in Archaeology, pp. 337–345.
Campaña, I., Benito-Calvo, A., Pérez-González, A., Ortega, A.I., Bermúdez de Castro, J.M., Carbonell, E., 2017. Pleistocene sedimentary facies of the Gran Dolina archaeo-paleoanthropological site (Sierra de Atapuerca, Burgos, Spain). Quat. Int. 433, 68–84. https://doi.org/10.1016/j.quaint.2015.04.023.
Canals, A., Galobart, À., 2003. Arqueoestratigrafía y reconstrucción de la dinámica sedimentaria en los yacimientos del Pleistoceno inferior de Incarcal I e Incarcal V. Paleontol. Evol. 34, 221–232.
Canals, A., Rodríguez, J., Sánchez, R., 2008. The 3COORsystem for data recording in archaeology. J. Anthropol. Sci. 86, 133–141.
Canals, A., Vallverdú, J., Carbonell, E., 2003. New archaeo-stratigraphic data for the TD6 level in relation to Homo antecessor (Lower Pleistocene) at the site of Atapuerca, north-central Spain. Geoarchaeol. An Int. J. 18, 481–504. https://doi.org/10.1002/gea.10071.
Capaldo, S.D., 1997. Experimental determinations of carcass processing by Plio-Pleistocene hominids and carnivores at FLK 22 (Zinjanthropus), Olduvai Gorge, Tanzania. J. Hum. Evol. 33, 555–597. https://doi.org/10.1006/jhev.1997.0150.
Carbonell, E., Mosquera, M., Ollé, A., Rodríguez, X.P., Sahnouni, M., Sala, R., Vergès, J.M., 2001. Structure morphotechnique de l'industrie lithique du Pléistocène inférieur et moyen d'Atapuerca (Burgos, Espagne). Anthropologie 105, 259–280. https://doi.org/10.1016/S0003-5521(01)80016-9.
Carrancho, A., Villalaín, J.J., Vallverdú, J., Carbonell, E., 2016. Is it possible to identify temporal differences among combustion features in Middle Palaeolithic palimpsests? The archaeomagnetic evidence: a case study from level O at the Abric Romaní rock-shelter (Capellades, Spain). Quat. Int. 417, 39–50. https://doi.org/10.1016/j.quaint.2015.12.083.
Cifuentes-Alcobendas, G., Domínguez-Rodrigo, M., 2019. Deep learning and taphonomy: high accuracy in the classification of cut marks made on fleshed and defleshed bones using convolutional neural networks. Sci. Rep. 9, 1–12. https://doi.org/10.1038/s41598-019-55439-6.
Cobo-Sánchez, L., 2020. Taphonomic and Spatial Study of the Archaeological Site DS from Bed I in Olduvai Gorge (Tanzania). Universidad Complutense de Madrid.
Cohen, J., 1960. A coefficient of agreement for nominal scales. Educ. Psychol. Meas. 20, 37–46. https://doi.org/10.1177/001316446002000104.
Cortes, C., Vapnik, V., 1995. Support-vector networks. Mach. Learn. 20, 273–297. https://doi.org/10.1109/64.163674.
Courtenay, L.A., Herranz-Rodrigo, D., González-Aguilera, D., Yravedra, J., 2021. Developments in data science solutions for carnivore tooth pit classification. Sci. Rep. 11, 1–15. https://doi.org/10.1038/s41598-021-89518-4.
Courtenay, L.A., Huguet, R., González-Aguilera, D., Yravedra, J., 2020. A hybrid geometric morphometric deep learning approach for cut and trampling mark classification. Appl. Sci. 10. https://doi.org/10.3390/app10010150.
Cuenca-Bescós, G., Rofes, J., Garcia-Pimienta, J., 2005. Environmental change across the Early-Middle Pleistocene transition: small mammalian evidence from the Trinchera Dolina cave, Atapuerca, Spain. Geol. Soc. Spec. Publ. 247, 277–286. https://doi.org/10.1144/GSL.SP.2005.247.01.16.
Cziesla, E., 1990. On refitting of stone artefacts. In: Cziesla, E., Eickhoff, S., Arts, N., Winter, D. (Eds.), The Big Puzzle: International Symposium on Refitting Stone Artefacts. Holos, Bonn, pp. 9–44.
de la Torre, I., Martínez-Moreno, J., Mora, R., 2012. When bones are not enough: lithic refits and occupation dynamics in the Middle Palaeolithic Level 10 of Roca dels Bous (Catalonia, Spain). In: Bones for Tools - Tools for Bones. The Interplay between Objects and Objectives, pp. 13–23.
de la Torre, I., Vanwezer, N., Benito-Calvo, A., Proffitt, T., Mora, R., 2019. Spatial and orientation patterns of experimental stone tool refits. Archaeol. Anthropol. Sci. 11, 4569–4584.
de Lombera-Hermida, A., Rodríguez-Álvarez, X.-P., Mosquera, M., Ollé, A., García-Medrano, P., Pedergnana, A., Terradillos-Bernal, M., López-Ortega, E., Bargalló, A., Rodríguez-Hidalgo, A., Saladié, P., Bermúdez de Castro, J.M., Carbonell, E., 2020. The dawn of the Middle Paleolithic in Atapuerca: the lithic assemblage of TD10.1 from Gran Dolina. J. Hum. Evol. 145. https://doi.org/10.1016/j.jhevol.2020.102812.
Deschamps, M., Zilhão, J., 2018. Assessing site formation and assemblage integrity through stone tool refitting at Gruta da Oliveira (Almonda karst system, Torres Novas, Portugal): a Middle Paleolithic case study. PLoS One. https://doi.org/10.1371/journal.pone.0192423.
Dibble, H.L., 1987. Measurement of artifact provenience with an electronic theodolite. J. Field Archaeol. 14, 249–254. https://doi.org/10.1179/009346987792208457.
Dibble, H.L., Holdaway, S.J., Lin, S.C., Braun, D.R., Douglass, M.J., Iovita, R., McPherron, S.P., Olszewski, D.I., Sandgathe, D., 2017. Major fallacies surrounding stone artifacts and assemblages. J. Archaeol. Method Theor 24, 813–851. https://doi.org/10.1007/s10816-016-9297-8.
Diez-Martín, F., Sánchez-Yustos, P., Uribelarrea, D., Domínguez-Rodrigo, M., Fraile-Márquez, C., Obregón, R.A., Díaz-Muñoz, I., Mabulla, A., Baquedano, E., Pérez-González, A., Bunn, H.T., 2014. New archaeological and geological research at SHK main site (Bed II, Olduvai Gorge, Tanzania). Quat. Int. 322–323, 107–128. https://doi.org/10.1016/j.quaint.2013.11.004.
Discamps, E., Bachellerie, F., Baoillet, M., Sitzia, L., 2019. The use of spatial taphonomy for interpreting pleistocene palimpsests: an interdisciplinary approach to the Châtelperronian and carnivore occupations at Cassenade (Dordogne, France). PaleoAnthropology 362–388. https://doi.org/10.4207/PA.2019.ART136.
Domínguez-Rodrigo, M., 2019. Successful classification of experimental bone surface modifications (BSM) through machine learning algorithms: a solution to the controversial use of BSM in paleoanthropology? Archaeol. Anthropol. Sci. 11, 2711–2725. https://doi.org/10.1007/s12520-018-0684-9.
Domínguez-Rodrigo, M., Baquedano, E., 2018. Distinguishing butchery cut marks from crocodile bite marks through machine learning methods. Sci. Rep. 8, 1–8. https://doi.org/10.1038/s41598-018-24071-1.
Dunnell, R.C., 1982. Science, social science, and common sense: the agonizing dilemma of modern archaeology. J. Anthropol. Res. 38, 1–25.
Duval, M., Arnold, L.J., Demuro, M., Parés, J.M., Campaña, I., Carbonell, E., Bermúdez de Castro, J.M., 2022. New chronological constraints for the lowermost stratigraphic unit of Atapuerca Gran Dolina (Burgos, N Spain). Quat. Geochronol. 71, 101292. https://doi.org/10.1016/j.quageo.2022.101292.
Elliot, T., Morse, R., Smythe, D., Norris, A., 2021. Evaluating machine learning techniques for archaeological lithic sourcing: a case study of flint in Britain. Sci. Rep. 11, 1–14. https://doi.org/10.1038/s41598-021-87834-3.
Falguères, C., Bahain, J.-J., Yokoyama, Y., Arsuaga, J.L., Bermudez De Castro, J.M., Carbonell, E., Bischoff, J.L., Dolo, J.M., 1999. Earliest humans in Europe: the age of TD6 Gran Dolina, Atapuerca, Spain. J. Hum. Evol. 37, 343–352. https://doi.org/10.1006/jhev.1999.0326.
Falguères, C., Bahain, J.-J., Yokoyama, Y., Bischoff, J.L., Arsuaga, J.L., Bermudez de Castro, J.M.B. De, Carbonell, E., Dolo, J.-M., 2001. Datation par RPE et U-TH des sites plèistocènes d'Atapuerca: sima de los Huesos, Trinchera Dolina et Trinchera Galería. Bilan gèochronologique. Anthropologie 105, 71–81. https://doi.org/10.1016/S0003-5521(01)80006-6.
Fernández-Laso, M.C., Rosell, J., Blasco, R., Vaquero, M., 2020. Refitting bones: spatial relationships between activity areas at the Abric Romaní Level M (Barcelona, Spain). J. Archaeol. Sci. Reports 29, 102188. https://doi.org/10.1016/j.jasrep.2019.102188.
Foley, R.A., 1981. Off-site archaeology: an alternative approach for the short-sited. In: Hodder, I., Isaac, G.L., Hammond, N. (Eds.), Pattern of the Past. Studies in Honour of David Clarke. Cambridge University Press, pp. 157–183.
Font, B., López-Polín, L., Ollé, A., 2010. Description and characterization of the natural alteration of chert artefacts from Atapuerca (Burgos, Spain), Cansaladeta (Tarragona, Spain) and Orgnac 3 (Ardèche, France). Ann. dell'Università di Ferrara. Mus. Sci. Nat. 6, 103–110. https://doi.org/10.15160/1824-2707/418.
Galanidou, N., 2000. Patterns in caves: foragers, horticulturists, and the use of space. J. Anthropol. Archaeol. 19, 243–275. https://doi.org/10.1006/jaar.1999.0362.
Gallotti, R., Mohib, A., Graoui, M. El, Sbihi-Alaoui, F.Z., Raynal, J.-P., 2011. GIS and intra-site spatial analyses: an integrated approach for recording and analyzing the fossil deposits at Casablanca prehistoric sites (Morocco). J. Geogr. Inf. Syst. 3, 373–381. https://doi.org/10.4236/jgis.2011.34036.
García-Antón, M.D., 2016. La captación, selección y gestión de recursos líticos en la Prehistoria: Una visión diacrónica del uso del territorio y sus recursos en el entorno de la sierra de Atapuerca (Burgos) durante el Pleistoceno inferior y medio. Universitat Rovira i Virgili.
Gil, E., Aguirre, E., Hoyos, M., 1987. Contexto estratigráfico. In: Aguirre, Emiliano, Carbonell, E., Bermúdez de Castro, J.M. (Eds.), El Hombre Fósil de Ibeas y El Pleistoceno de La Sierra de Atapuerca. Junta de Castilla y León, Valladolid,

pp. 45–47.
Giusti, D., Arzarello, M., 2016. The need for a taphonomic perspective in spatial analysis: formation processes at the Early Pleistocene site of Pirro Nord (P13), Apricena, Italy. J. Archaeol. Sci. Reports 8, 235–249. https://doi.org/10.1016/j.jasrep.2016.06.014.
González-Molina, I., Jiménez-García, B., Maíllo-Fernández, J.M., Baquedano, E., Domínguez-Rodrigo, M., 2020. Distinguishing discoid and centripetal levallois methods through machine learning. PLoS One 15, 15–18. https://doi.org/10.1371/journal.pone.0244288.
Goodfellow, I., Bengio, Y., Courville, A., 2016. Deep Learning. MIT Press, Cambridge.
Gowlett, J.A.J., 1997. High definition archaeology. ideas and evaluation. World Archaeol. 29, 152–171.
Grove, M., Blinkhorn, J., 2020. Neural networks differentiate between Middle and Later stone age lithic assemblages in Eastern Africa. PLoS One 15, 1–27. https://doi.org/10.1371/journal.pone.0237528.
Harding, J., 2005. Rethinking the great divide: long-term structural history and the temporality of event. Nor. Archaeol. Rev. 38, 88–101. https://doi.org/10.1080/00293650510032707.
Henry, D., 2012. The palimpsest problem, hearth pattern analysis, and Middle Paleolithic site structure. Quat. Int. 247, 246–266. https://doi.org/10.1016/j.quaint.2010.10.013.
Hofman, J.L., 1986. Vertical movement of artifacts in alluvial and stratified deposits. Curr. Anthropol. 27, 163–171. https://doi.org/10.1086/203414.
Holdaway, S.J., Wandsnider, L., 2008. Time in Archaeology: Time Perspectivism Revisited. University of Utah Press, Salt Lake City, USA.
Jalandoni, A., Zhang, Y., Zaidi, N.A., 2022. On the use of Machine Learning methods in rock art research with application to automatic painted rock art identification. J. Archaeol. Sci. 144, 105629. https://doi.org/10.1016/J.JAS.2022.105629.
Julien, M.A., Rivals, F., Serangeli, J., Bocherens, H., Conard, N.J., 2015. A new approach for deciphering between single and multiple accumulation events using intra-tooth isotopic variations: application to the Middle Pleistocene bone bed of Schöningen 13 II-4. J. Hum. Evol. 89, 114–128. https://doi.org/10.1016/j.jhevol.2015.02.012.
Kowalewski, M., 1996. Time-Averaging, overcompleteness, and the geological record. J. Geol. 104, 317–326.
Kuhn, M., 2020. Caret: classification and Regression Training. R package version 6.0-86. https://cran.r-project.org/package=caret.
Kuhn, S.L., Clark, A.E., 2015. Artifact densities and assemblage formation: evidence from tabun cave. J. Anthropol. Archaeol. 38, 8–16. https://doi.org/10.1016/j.jaa.2014.09.002.
Kvamme, K.L., 1997. Patterns and models of debitage dispersal in percussion flaking. Lithic Technol. 22, 122–138. https://doi.org/10.1080/01977261.1997.11754538.
LaMotta, V.M., Schiffer, M.B., 1999. Formation processes of house floor assemblages. In: Allison, P. (Ed.), The Archaeology of Household Activities. Routledge, London, pp. 19–29.
Landis, R.J., Koch, G.G., 1977. The measurement of observer agreement for categorical data. Biometrics 33, 159–174. https://doi.org/10.2307/2529310.
Leierer, L., Jambrina-Enríquez, M., Herrera-Herrera, A.V., Connolly, R., Hernández, C.M., Galván, B., Mallol, C., 2019. Insights into the timing, intensity and natural setting of Neanderthal occupation from the geoarchaeological study of combustion structures: a micromorphological and biomarker investigation of El Salt, unit Xb, Alcoy, Spain. PLoS One. https://doi.org/10.1371/journal.pone.0214955.
López-Ortega, E., Bargalló, A., de Lombera-Hermida, A., Mosquera, M., Ollé, A., Rodríguez, X.P., 2017. Quartz and quartzite refits at Gran Dolina (Sierra de Atapuerca, Burgos): connecting lithic artefacts in the Middle Pleistocene unit of TD10.1. Quat. Int. 433, 85–102. https://doi.org/10.1016/j.quaint.2015.09.026.
López-Ortega, E., Rodríguez-Álvarez, X.P., Ollé, A., Lozano, S., 2019. Lithic refits as a tool to reinforce postdepositional analysis. Archaeol. Anthropol. Sci. 11, 4555–4568. https://doi.org/10.1007/s12520-019-00808-5.
Lucas, G., 2012. Understanding the Archaeological Record, Understanding the Archaeological Record. Cambridge University Press. https://doi.org/10.1017/CBO9780511845772.
Luzón, C., Yravedra, J., Courtenay, L.A., Saarinen, J., Blain, H.A., Demiguel, D., Viranta, S., Azanza, B., José, J., Alba, R., Herranz-Rodrigo, D., Serrano-Ramos, A., Solano, J.A., Oms, O., Agustí, J., Fortelius, M., Jiménez-Arenas, J.M., 2021. Taphonomic and spatial analyses from the early pleistocene site of Venta Micena 4 (Orce , Guadix - Gaza basin , southern Spain). Sci. Rep. 4, 1–17. https://doi.org/10.1038/s41598-021-93261-1.
Lyman, L.R., 2003. The influence of time averaging and space averaging on the application of foraging theory in zooarchaeology. J. Archaeol. Sci. 30, 595–610. https://doi.org/10.1016/S0305-4403(02)00236-4.
Machado, J., Hernández, C.M., Mallol, C., Galván, B., 2013. Lithic production, site formation and Middle Palaeolithic palimpsest analysis: in search of human occupation episodes at Abric del Pastor Stratigraphic Unit IV (Alicante, Spain). J. Archaeol. Sci. 40, 2254–2273. https://doi.org/10.1016/j.jas.2013.01.002.
Machado, J., Mallol, C., Hernández, C.M., 2015. Insights into eurasian Middle Paleolithic settlement dynamics: the palimpsest problem. In: Conard, N.J., Delagnes, A. (Eds.), Settlement Dynamics of the Middle Paleolithic and Middle Stone Age. Tübingen Publications in Prehistory, Tübingen, pp. 361–382.
Machado, J., Mayor, A., Hernández, C.M., Galván, B., 2019. Lithic refitting and the analysis of Middle Palaeolithic settlement dynamics: a high-temporal resolution example from El Pastor rock shelter (Eastern Iberia). Archaeol. Anthropol. Sci. 11, 4539–4554. https://doi.org/10.1007/s12520-019-00859-8.
Malinsky-Buller, A., Hovers, E., Marder, O., 2011. Making time: "Living floors", "palimpsests" and site formation processes - A perspective from the open-air Lower Paleolithic site of Revadim Quarry, Israel. J. Anthropol. Archaeol. 30, 89–101. https://doi.org/10.1016/j.jaa.2010.11.002.
Mallol, C., Carbonell, E., 2008. The collapse of Gran Dolina cave, Sierra de Atapuerca, Spain: site Formation Processes of layer TD10-1. Geoarchaeology 23, 13–41. https://doi.org/10.1002/GEA.
Mallol, C., Hernández, C., 2016. Advances in palimpsest dissection. Quat. Int. 417, 1–2. https://doi.org/10.1016/j.quaint.2016.09.021.
Mallol, C., Hernández, C., Cabanes, D., Sistiaga, A., Machado, J., Rodríguez, Á., Pérez, L., Galván, B., 2013. The black layer of Middle Palaeolithic combustion structures. Interpretation and archaeostratigraphic implications. J. Archaeol. Sci. 40, 2515–2537. https://doi.org/10.1016/j.jas.2012.09.017.
Marín, J., Rodríguez-Hidalgo, A., Vallverdú, J., Gómez de Soler, B., Rivals, F., Rabuñal, J.R., Pineda, A., Chacón, M.G., Carbonell, E., Saladié, P., 2019. Neanderthal logistic mobility during MIS3: zooarchaeological perspective of Abric Romaní Level P (Spain). Quat. Sci. Rev. 225, 10633. https://doi.org/10.1016/j.quascirev.2019.106033.
Márquez, B., Ollé, A., Sala, R., Vergès, J.M., 2001. Perspectives methodologiques de l'analyse fonctionnelle des ensembles lithiques du Pléistocène inférieur et moyen d'Atapuerca (Burgos, Espagne). L'Anthropologie 105, 281–299.
Martín-Perea, D.M., Courtenay, L.A., Domingo, M.S., Morales, J., 2020. Application of artificially intelligent systems for the identification of discrete fossiliferous levels. PeerJ 2020, 1–25. https://doi.org/10.7717/peerj.8767.
Martín-Perea, D.M., Domingo, M.S., Cantero, E., Courtenay, L.A., Valenciano, A., Sualdea, L.R., Abella, J., Morales, J., 2021a. Recurring taphonomic processes in the carnivoran-dominated late miocene assemblages of batallones-3, madrid basin, Spain. Lethaia 54, 871–890. https://doi.org/10.1111/let.12445.
Martín-Perea, D.M., Morales, J., Cantero, E., Courtenay, L.A., Hernández Fernández, M., Domingo, M.S., 2021b. Taphonomic analysis of Batallones-10, a Late Miocene drought-induced mammalian assemblage (Madrid basin, Spain) within the Cerro de los Batallones complex. Palaeogeogr. Palaeoclimatol. Palaeoecol. 578. https://doi.org/10.1016/j.palaeo.2021.110576.
Martínez-Moreno, J., Mora Torcal, R., Roy Sunyer, M., Benito-Calvo, A., 2016. From site formation processes to human behaviour: towards a constructive approach to depict palimpsests in Roca dels Bous. Quat. Int. 417, 82–93. https://doi.org/10.1016/j.quaint.2015.09.038.
Mas, B., Allué, E., Alonso, E.S., Vaquero, M., 2021. From forest to settlement: Magdalenian hunter-gatherer interactions with the wood vegetation environment based on anthracology and intra-site spatial distribution. Archaeol. Anthropol. Sci. 13. https://doi.org/10.1007/s12520-020-01264-2.
Mcpherron, S.J.P., Dibble, H.L., Goldberg, P., 2005. Z. Geoarchaeology An Int. J. 20, 243–262. https://doi.org/10.1002/gea.20048.
Menéndez Granda, D.L., 2009. La transición del Modo 2 al Modo 3 vista a través de la industria lítica de Gran Dolina TD10 (Atapuerca, Burgos) y Orgnac 3 (Ardéche, Francia). Desarrollo tecnológico y posibles implicaciones ocupacionales de los conjuntos. Universitat Rovira i Virgili.
Meyer, D., Dimitriadou, E., Hornik, K., Weingessel, A., Leisch, F., 2021. e1071: Misc Functions of the Department of Statistics, Probability Theory Group. R Package Version 1.7-5. https://cran.r-project.org/package=e1071.
Moclán, A., Domínguez-Rodrigo, M., Yravedra, J., 2019. Classifying agency in bone breakage: an experimental analysis of fracture planes to differentiate between hominin and carnivore dynamic and static loading using machine learning (ML) algorithms. Archaeol. Anthropol. Sci. 11, 4663–4680. https://doi.org/10.1007/s12520-019-00815-6.
Mora Torcal, R., Roy Sunyer, M., Martínez-Moreno, J., Benito-Calvo, A., Samper Carro, S., 2020. Inside the palimpsest: identifying short occupations in the 497D level of Cova Gran (Iberia). In: Cascalheira, J., Picin, A. (Eds.), Short-Term Occupations in Paleolithic Archaeology. Springer International Publishing, pp. 39–69. https://doi.org/10.1007/978-3-030-27403-0.
Moreno, D., Falguères, C., Pérez-González, A., Voinchet, P., Ghaleb, B., Despriée, J., Bahain, J.-J., Sala, R., Carbonell, E., Bermúdez de Castro, J.M., Arsuaga, J.L., 2015. New radiometric dates on the lowest stratigraphical section (TD1 to TD6) of Gran Dolina site (Atapuerca, Spain). Quat. Geochronol. 30, 535–540. https://doi.org/10.1016/j.quageo.2015.05.007.
Morrow, T.M., 1996. Lithic refitting and archaeological site formation processes. In: Odell, G.H. (Ed.), Stone Tools. Interdisciplinary Contributions to Archaeology. Springer, Boston, pp. 345–373.
Nash, B.S., Prewitt, E.R., 2016. The use of artificial neural networks in projectile point typology. Lithic Technol. 41, 194–211. https://doi.org/10.1080/01977261.2016.1184876.
Newcomer, M.H., Sieveking, G.D.G., 1980. Experimental flake scatter-patterns: a new interpretative technique. J. Field Archaeol. 7, 345–352. https://doi.org/10.1179/009346980791505392.
Ngoloyi, N.M., Dumoncel, J., Thackeray, J.F., Braga, J., 2020. A new method to evaluate 3D spatial patterns within early hominin-bearing sites. An example from Kromdraai (Gauteng Province, South Africa). J. Archaeol. Sci. Rep. 32, 102376. https://doi.org/10.1016/j.jasrep.2020.102376.
Obregón Labrador, R.A., 2012. Estratigrafía cultural en el nivel TD10-1 de Gran Dolina, Sierra de Atapuerca (Burgos): Secuencia arqueoestratigráfica de los asentamientos contenidos en sedimento homogéneo. Universidad de Burgos.
Ollé, A., Mosquera, M., Rodríguez, X.P., de Lombera-Hermida, A., García-Antón, M.D., García-Medrano, P., Peña, L., Menéndez, L., Navazo, M., Terradillos, M., Bargalló, A., Márquez, B., Sala, R., Carbonell, E., 2013. The Early and Middle Pleistocene technological record from Sierra de Atapuerca (Burgos, Spain). Quat. Int. 295, 138–167. https://doi.org/10.1016/j.quaint.2011.11.009.

Olszewski, T., 1999. Taking advantage of time-averaging. Paleobiology 25, 226–238.
Orellana Figueroa, J.D., Reeves, J.S., McPherron, S.P., Tennie, C., 2021. A proof of concept for machine learning-based virtual knapping using neural networks. Sci. Rep. 11, 1–12. https://doi.org/10.1038/s41598-021-98755-6.
Orengo, H.A., Conesa, F.C., Garcia-Molsosa, A., Lobo, A., Green, A.S., Madella, M., Petrie, C.A., 2020. Automated detection of archaeological mounds using machine-learning classification of multisensor and multitemporal satellite data. Proc. Natl. Acad. Sci. U.S.A. 117, 18240–18250. https://doi.org/10.1073/pnas.2005583117.
Ortega, A.I., Benito-Calvo, A., Pérez-González, A., Martín-Merino, M.A., Pérez-Martínez, R., Parés, J.M., Aranburu, A., Arsuaga, J.L., Bermúdez de Castro, J.M., Carbonell, E., 2013. Evolution of multilevel caves in the Sierra de Atapuerca (Burgos, Spain) and its relation to human occupation. Geomorphology 196, 122–137. https://doi.org/10.1016/j.geomorph.2012.05.031.
Parés, J.M., Álvarez, C., Sier, M., Moreno, D., Duval, M., Woodhead, J.D., Ortega, A.I., Campaña, I., Rosell, J., Bermúdez de Castro, J.M., Carbonell, E., 2018. Chronology of the cave interior sediments at Gran Dolina archaeological site, Atapuerca (Spain). Quat. Sci. Rev. 186, 1–16. https://doi.org/10.1016/j.quascirev.2018.02.004.
Parés, J.M., Pérez-González, A., 1999. Magnetochronology and stratigraphy at Gran Dolina section, Atapuerca (Burgos, Spain). J. Hum. Evol. 37, 325–342. https://doi.org/10.1006/jhev.1999.0331.
Pedergnana, A., Ollé, A., 2020. Use-wear analysis of the late Middle Pleistocene quartzite assemblage from the Gran Dolina site, TD10.1 subunit (Sierra de Atapuerca, Spain). Quat. Int. 569–570, 181–211. https://doi.org/10.1016/j.quaint.2019.11.015.
Pérez-González, A., Parés, J.M., Carbonell, E., Aleixandre, T., Ortega, A.I., Benito-Calvo, A., Martín-Merino, M.A., 2001. Géologie de la Sierra de Atapuerca et stratigraphie des remplissages karstiques de Galería et Dolina (Burgos, Espagne). Anthropologie 105, 27–43.
Perreault, C., 2019. The Quality of the Archaeological Record. University of Chicago Press, Chicago and London. https://doi.org/10.7208/chicago/9780226631011.003.0005.
Pettitt, P.B., 1997. High resolution Neanderthals? interpreting Middle Palaeolithic intrasite spatial data. World Archaeol. 29, 208–224. https://doi.org/10.1080/00438243.1997.9980374.
Reeves, J.S., McPherron, S.P., Aldeias, V., Dibble, H.L., Goldberg, P., Sandgathe, D., Turq, A., 2019. Measuring spatial structure in time-averaged deposits insights from Roc de Marsal, France. Archaeol. Anthropol. Sci. 11, 5743–5762. https://doi.org/10.1007/s12520-019-00871-y.
Rivals, F., Moncel, M.H., Patou-Mathis, M., 2009a. Seasonality and intra-site variation of Neanderthal occupations in the Middle Palaeolithic locality of Payre (Ardèche, France) using dental wear analyses. J. Archaeol. Sci. 36, 1070–1078. https://doi.org/10.1016/j.jas.2008.12.009.
Rivals, F., Schulz, E., Kaiser, T.M., 2009b. A new application of dental wear analyses: estimation of duration of hominid occupations in archaeological localities. J. Hum. Evol. 56, 329–339. https://doi.org/10.1016/j.jhevol.2008.11.005.
Rodríguez-Hidalgo, A., 2016. Subsistence dynamics during the lower paleolithic in Gran Dolina cave (Atapuerca, Spain). Mitteilungen der Gesellschaft für Urgeschichte 25, 11–48.
Rodríguez-Hidalgo, A., 2015. Dinámicas Subsistenciales durante el Pleistoceno Medio en la sierra de Atapuerca: Los conjuntos arqueológicos de TD10.1 y TD10.2. Universitat Rovira i Virgili.
Rodríguez-Hidalgo, A., Rivals, F., Saladié, P., Carbonell, E., 2016. Season of bison mortality in TD10.2 bone bed at Gran Dolina site (Atapuerca): integrating tooth eruption, wear, and microwear methods. J. Archaeol. Sci. Rep. 6, 780–789. https://doi.org/10.1016/j.jasrep.2015.11.033.
Rodríguez-Hidalgo, A., Saladié, P., Ollé, A., Arsuaga, J.L., Bermúdez de Castro, J.M., Carbonell, E., 2017. Human predatory behavior and the social implications of communal hunting based on evidence from the TD10.2 bison bone bed at Gran Dolina (Atapuerca, Spain). J. Hum. Evol. 105, 89–122. https://doi.org/10.1016/j.jhevol.2017.01.007.
Rodríguez-Hidalgo, A., Saladié, P., Ollé, A., Carbonell, E., 2015. Hominin subsistence and site function of TD10.1 bone bed level at Gran Dolina site (Atapuerca) during the late Acheulean. J. Quat. Sci. 30, 679–701. https://doi.org/10.1002/jqs.2815.
Rodríguez, J., Burjachs, F., Cuenca-Bescós, G., García, N., Van der Made, J., Pérez-González, A., Blain, H.A., Expósito, I., López-García, J.M., García-Antón, M.D., Allué, E., Cáceres, I., Huguet, R., Mosquera, M., Ollé, A., Rosell, J., Parés, J.M., Rodríguez-Álvarez, X.P., Díez, C., Rofes, J., Sala, R., Saladié, P., Vallverdú, J., Bennàsar, M.L., Blasco, R., Bermúdez de Castro, J.M., Carbonell, E., 2011. One million years of cultural evolution in a stable environment at Atapuerca (Burgos, Spain). Quat. Sci. Rev. 30, 1396–1412. https://doi.org/10.1016/j.quascirev.2010.02.021.
Roebroeks, W., 1988. From Find Scatters to Early Hominid Behaviour: a Study of Middle Palaeolithic Riverside Settlements at Maastricht-Belvédère (The Netherlands), Analecta Praehistorica Leidensia. Leiden university Press, Leiden.
Romagnoli, F., Nishiaki, Y., Rivals, F., Vaquero, M., 2018. Time uncertainty, site formation processes, and human behaviours: new insights on old issues in High-Resolution Archaeology. Quat. Int. 474, 99–102. https://doi.org/10.1016/j.quaint.2018.04.033.
Romagnoli, F., Vaquero, M., 2019. The challenges of applying refitting analysis in the Palaeolithic archaeology of the twenty-first century: an actualised overview and future perspectives. Archaeol. Anthropol. Sci. 11, 4387–4396. https://doi.org/10.1007/s12520-019-00888-3.
Romagnoli, F., Vaquero, M., 2016. Quantitative stone tools intra-site point and orientation patterns of a Middle Paleolithic living floor: a GIS multi-scalar spatial and temporal approach. Quartar 63, 47–60.
Rosell, J., 2002. Patrons d'aprofitament de les biomasses animals durant el Pleistocè inferior i mig (sierra de Atapuerca, Burgos) superior (Abric Romaní, Barcelona). Universitat Rovira i Virgili.
Rosell, J., Blasco, R., Fernández-Laso, M.C., Vaquero, M., Carbonell, E., 2012. Connecting areas: faunal refits as a diagnostic element to identify synchronicity in the Abric Romaní archaeological assemblages. Quat. Int. 252, 56–67. https://doi.org/10.1016/j.quaint.2011.02.019.
Roy Sunyer, M., 2016. Deconstructing archaeological palimpsests: applicability of GIS algorithms for the automated generation of cross sections. In: Campana, S., Scopigno, R., Carpentiero, G., Cirillo, M. (Eds.), Proceedings of the 43rd Annual Conference on Computer Applications and Quantitative Methods in Archaeology, ume 1. Archaeopress, Oxford, pp. 407–414.
Saladié, P., Rodríguez-Hidalgo, A., Marín, J., Vallverdú, J., Carbonell, E., 2018. The top of the Gran Dolina (Atapuerca, Spain) sequence: a zooarchaeological and occupational perspective. Quat. Sci. Rev. 195, 48–71. https://doi.org/10.1016/j.quascirev.2018.07.010.
Sánchez-Romero, L., Canals, A., Pérez-González, A., Márquez, B., Mosquera, M., Karampaglidis, T., Arsuaga, J.L., Baquedano, E., 2017. Breaking the palimpsest: an approach to the cultural sequence of Neanderthal occupation at the Navalmaíllo rockshelter, Pinilla del Valle (Spain). Trab. Prehist. 74, 225. https://doi.org/10.3989/tp.2017.12192.
Sañudo, P., Blasco, R., Fernández Peris, J., 2016. Site formation dynamics and human occupations at Bolomor Cave (Valencia, Spain): an archaeostratigraphic analysis of levels I to XII (100–200 ka). Quat. Int. 417, 94–104. https://doi.org/10.1016/j.quaint.2015.09.044.
Sañudo, P., Vallverdú, J., Canals, A., 2012. Spatial patterns in level J. In: Carbonell, E. (Ed.), High Resolution Archaeology and Neanderthal Behavior: Time and Space in Level J of Abric Romaní (Capellades, Spain). Springer, pp. 313–372. https://doi.org/10.1007/978-94-007-3922-2.
Schiffer, M.B., 1987. Formation Processes of the Archaeological Record. University of New Mexico Press, Albuquerque.
Schiffer, M.B., 1985. Is there a "Pompeii Premise" in archaeology? J. Anthropol. Res. 41, 18–41.
Schiffer, M.B., 1983. Toward the identification of formation processes. Am. Antiq. 48, 675–706. https://doi.org/10.2307/279771.
Schiffer, M.B., 1975. Archaeology as behavioral science. Am. Anthropol. 77, 836–848. https://doi.org/10.1525/aa.1975.77.4.02a00060.
Schiffer, M.B., 1972. Archaeological context and systemic context. Am. Antiq. 37, 156–165.
Shott, M.J., 2008. Lower Paleolithic industries, time, and the meaning of assemblage variation. In: Holdaway, S.J., Wandsnider, L. (Eds.), Time in Archaeology: Time Perspectivism Revisited, pp. 46–60.
Sisk, M.L., Shea, J.J., 2008. Intrasite spatial variation of the Omo Kibish Middle Stone Age assemblages: artifact refitting and distribution patterns. J. Hum. Evol. 55, 486–500. https://doi.org/10.1016/j.jhevol.2008.05.016.
Smith, M.E., 1992. Braudel's temporal rhythms and chronology theory in archaeology. In: Knapp, B. (Ed.), Archaeology, Annales , and Ethnohistory. Cambridge University Press, New York, pp. 23–34. https://doi.org/10.1017/cbo9780511759949.003.
Soto, M., Arteaga-Brieba, A., Mosquera, M., Ollé, A., Vallverdú, J., 2021. Neogene chert exploitation at sub-unit TD10.2 (Atapuerca, Burgos). In: Gómez de Soler, B., Soto, M., Chacón, M.G., Soares, M. (Eds.), Rock and Roll: 13th International Symposium on Knappable Materials. Tarragona, p. 90.
Spagnolo, V., Marciani, G., Aureli, D., Berna, F., Boscato, P., Ranaldo, F., Ronchitelli, A., 2016. Between hearths and volcanic ash: the SU 13 palimpsest of the Oscurusciuto rock shelter (Ginosa – southern Italy): analytical and interpretative questions. Quat. Int. 417, 105–121. https://doi.org/10.1016/j.quaint.2015.11.046.
Stein, J.K., 2001. A review of site formation processes and their relevance to geoarchaeology. In: Goldberg, P., Holliday, V.T., Ferring, R. (Eds.), Earth Sciences and Archaeology. Plenum Publishers, New York, pp. 37–51. https://doi.org/10.1007/978-1-4615-1183-0_2.
Stern, N., 2008. Time averaging and the structure of late pleistocene archaeological deposits in Southwest Tasmania. In: Time in Archaeology: Time Perspectivism Revisited, pp. 134–148.
Stern, N., 1994. The implications of time-averaging for reconstructing the land-use patterns of early tool-using hominids. J. Hum. Evol. 27, 89–105.
Sullivan, A.P., 2008. Time perspectivism and the interpretive potential of palimpsests: theoretical and methodological considerations of assemblage formation history and contemporaneity. In: Holdaway, S.J., Wandsnider, L. (Eds.), Time in Archaeology: Time Perspectivism Revisited. University of Utah Press, Salt Lake City, USA, pp. 31–45.
Sumner, T.A., Kuman, K., 2014. Refitting evidence for the stratigraphic integrity of the Kudu Koppie Early to Middle Stone Age site, northern Limpopo province, South Africa. Quat. Int. 343, 169–178. https://doi.org/10.1016/j.quaint.2014.04.017.
Terradillos Bernal, M., Díez-Fernández, J.-C., 2012. La transition entre les Modes 2 et 3 en Europe : le rapport sur les gisements du Plateau Nord (Péninsule Ibérique). Anthropologie 116, 348–363. https://doi.org/10.1016/j.anthro.2012.06.001.
Thabeng, O.L., Merlo, S., Adam, E., 2019. High-resolution remote sensing and advanced classification techniques for the prospection of archaeological sites' markers: the case of dung deposits in the Shashi-Limpopo Confluence area (southern Africa). J. Archaeol. Sci. 102, 48–60. https://doi.org/10.1016/

j.jas.2018.12.003.
Vallverdú, J., 2017. Soil-stratigraphy in the cave entrance deposits of Middle Pleistocene age at the Trinchera del Ferrocarril sites (Sierra de Atapuerca, Spain). Quat. Int. 433, 199–210. https://doi.org/10.1016/j.quaint.2015.09.031.
Vallverdú, J., 2013. Estudio arqueo-estratigráfico del subnivel TD10-Sup de Gran Dolina (Sierra de Atapuerca), Not published.
Vallverdú, J., Courty, M.A., 2012. Microstratigraphic analysis of level J deposits: a dual paleoenvironmental-paleoethnographic contribution to paleolithic archeology at the abric romaní. In: Carbonell i Roura, E. (Ed.), High Resolution Archaeology and Neanderthal Behavior. Springer, pp. 77–133. https://doi.org/10.1007/978-94-007-3922-2_4.
Vaquero, M., 2008. The history of stones: behavioural inferences and temporal resolution of an archaeological assemblage from the Middle Palaeolithic. J. Archaeol. Sci. 35, 3178–3185. https://doi.org/10.1016/j.jas.2008.07.006.
Vaquero, M., Chacón, M.G., García-Antón, M.D., Gómez de Soler, B., Martínez, K., Cuartero, F., 2012. Time and space in the formation of lithic assemblages: the example of Abric Romaní Level. J. Quat. Int. 247, 162–181. https://doi.org/10.1016/j.quaint.2010.12.015.
Vaquero, M., Fernández-Laso, M.C., Chacón, M.G., Romagnoli, F., Rosell, J., Sañudo, P., 2017. Moving things: comparing lithic and bone refits from a Middle Paleolithic site. J. Anthropol. Archaeol. 48, 262–280. https://doi.org/10.1016/j.jaa.2017.09.001.
Vidal-Matutano, P., 2017. Firewood and hearths: middle palaeolithic woody taxa distribution from El Salt, stratigraphic unit Xb (eastern Iberia). Quat. Int. 457, 74–84. https://doi.org/10.1016/j.quaint.2016.07.040.
Villa, P., 1982. Conjoinable pieces and site formation processes. Am. Antiq. 47, 276–290.
Wandsnider, L.A., 2008. Time-averaged deposits and multitemporal processes in the Wyoming Basin, Intermontane North America: a preliminary consideration of land tenure in terms of occupation frequency and integration. In: Holdaway, S.J., Wandsnider, L. (Eds.), Time in Archaeology: Time Perspectivism Revisited. The University of Utah Press, Salt Lake City, USA, pp. 61–93.
Way, A.M., 2018. A behavioral approach to cumulative palimpsests: an example from Weereewaa (Lake George), Australia. J. Anthropol. Archaeol. 52, 59–70. https://doi.org/10.1016/j.jaa.2018.09.005.
Wood, W.R., Johnson, D.L., 1978. A survey of disturbance processes in archaeological site formation. Adv. Archaeol. Method Theor. 1, 315–381. https://doi.org/10.2307/20170136.
Yravedra, J., Domínguez-Rodrigo, M., Santonja, M., Rubio-Jara, S., Panera, J., Pérez-González, A., Uribelarrea, D., Egeland, C., Mabulla, A.Z.P., Baquedano, E., 2016. The larger mammal palimpsest from TK (Thiongo Korongo), bed II, Olduvai gorge, Tanzania. Quat. Int. 417, 3–15. https://doi.org/10.1016/j.quaint.2015.04.013.
Zorrilla-Revilla, G., Vidal-Cordasco, M., Prado-Nóvoa, O., Terradillos-Bernal, M., 2021. Know-how, or how knapping experience can affect a prehistoric lithic workshop. Lithic Technol. 1–15. https://doi.org/10.1080/01977261.2021.1911207, 0.